

Western Kentucky University

TopSCHOLAR®

Masters Theses & Specialist Projects

Graduate School

Summer 2021

Cellular Toxicity of Malonato (Ethylenediamine) Platinum (II) In Models of Cancer

Sidikat Olanrewaju Olajuwon

Western Kentucky University, sidikat.olajuwon699@topper.wku.edu

Follow this and additional works at: <https://digitalcommons.wku.edu/theses>



Part of the [Biochemistry Commons](#), [Cancer Biology Commons](#), [Structural Biology Commons](#), and the [Toxicology Commons](#)

Recommended Citation

Olajuwon, Sidikat Olanrewaju, "Cellular Toxicity of Malonato (Ethylenediamine) Platinum (II) In Models of Cancer" (2021). *Masters Theses & Specialist Projects*. Paper 3521.

<https://digitalcommons.wku.edu/theses/3521>

This Thesis is brought to you for free and open access by TopSCHOLAR®. It has been accepted for inclusion in Masters Theses & Specialist Projects by an authorized administrator of TopSCHOLAR®. For more information, please contact topscholar@wku.edu.

CELLULAR TOXICITY OF MALONATO(ETHYLENEDIAMINE)PLATINUM(II)
IN MODELS OF CANCER

A Thesis
Presented to
The Faculty of the Department of Chemistry
Western Kentucky University
Bowling Green, Kentucky

In Partial Fulfillment
Of the Requirements for the Degree
Master of Science

By
Sidikat Olanrewaju Olajuwon

August 2021

CELLULAR TOXICITY OF MALONATO(ETHYLENEDIAMINE)PLATINUM(II) IN
MODELS OF CANCER

Date Recommended 6/28/2021

B. Blairanne Williams Digitally signed by B. Blairanne Williams
Date: 2021.07.06 08:38:14 -05'00'

Blairanne Williams, Director of Thesis

Kevin Williams Digitally signed by Kevin Williams
DN: cn=Kevin Williams, o=Western Kentucky University,
ou=Department of Chemistry, email=kevin.williams@wku.edu,
c=US
Date: 2021.07.06 08:47:38 -05'00'

Kevin Williams

Moon-Soo Kim Digitally signed by Moon-Soo Kim
Date: 2021.07.08 23:30:09 +09'00'

Moon-Soo Kim



Associate Provost for Research and Graduate Education

I dedicate this thesis to my lovely parents, Alaba Mutiu and Sabirat Aina Olajuwon, who
have always been my backbone.

ACKNOWLEDGEMENTS

First, I would like to express my profound gratitude to my research advisor and mentor, Dr. Blairanne Williams for her mentorship, and support over the course of my graduate studies. I am really grateful for the time, effort, and patience she devoted towards my scientific development to help become a better scientist. I am forever grateful!

I would also like to acknowledge members of my thesis committee, Dr. Kevin Williams, and Dr. Moon-Soo Kim for accepting to be on my committee and working closely with me on my thesis and providing helpful insights and feedbacks during my thesis and defense process.

I would like to say ‘A Big Thank You’ to the Department of Chemistry, Ogden College of Science and Engineering, Graduate School, and International Student Office for making WKU a place to call home. Also, I am indeed grateful for granting me all available opportunities including graduate assistantships and funding to conduct my research.

I really want to appreciate both Ms. Haley Smith for always assisting me with the administrative part of being a graduate student and Ms. Alicia Pesterfield for always assisting me with stockroom requests during my teaching and research assistant duties. Thank you both for all you do for the Department of chemistry!

I would like to acknowledge the Kentucky Biomedical Research Infrastructure Network and INBRE (formerly KBRIN) for the grant support of our lab’s research project. Additionally, I want to thank Kentucky INBRE core at the University of Kentucky, Zachary Steckler for working me through during my thesis data analysis.

A special thank you to my awesome colleagues in Dr. B. Williams lab for their team work and supports. Also, I want to thank Vanesa Veletanlic and Megan Hall for allowing me to use their data for comparison for my thesis.

Lastly, I want to thank my wonderful family and friends for their enormous support during my graduate program and completion of my thesis. I really appreciate all the care, prayers, moral, and financial supports you all showered me with. I am indeed grateful for having you all. THANK YOU!!!

TABLE OF CONTENTS

	<u>Pages</u>
1. Introduction	
1.1. Platinum Chemotherapy.....	1
1.1.1. The Discovery of Cisplatin.....	1
1.1.2. FDA Approved Platinum Chemotherapy.....	3
1.2. Mechanisms of Platinum-Initiated Cell Deaths.....	5
1.2.1. Formation of Platinum-DNA Adduct.....	5
1.2.2. Accumulation of Platinum by Membrane Transporters.	7
1.2.2.1. Cellular Uptake of Platinum.....	9
1.2.2.2. Cellular Efflux of Platinum.....	11
1.3. Novel Platinum Compounds.....	12
2. Materials and Methods	
2.2. Cell Culture and Reagents.....	14
2.3. Platinum Compounds.....	15
2.4. Cell Growth Curves.....	16
2.5. MTT Assay.....	17
2.6. Statistical Analysis.....	19
3. Results	
3.2. Platinum Cellular Response.....	20
3.2.1. Pt(en)mal Cellular Response.....	20
3.2.2. Pt(en)CBDCA Cellular Response.....	24
3.2.3. Pt(en)Cl ₂ Cellular Response.....	26

	<u>Pages</u>
3.2.4. Carboplatin Cellular Response.....	29
3.2.5. IC ₅₀ Values.....	31
3.3. Effects of Leaving Ligand Differences on Cellular Responses....	33
3.3.1. Effects of Leaving Ligand in HEK293 Cell Line.....	33
3.3.2. Effects of Leaving Ligand in HT-29 Cell Line.....	34
3.3.3. Effects of Leaving Ligand in A549 Cell Line.....	36
3.3.4. Effects of Leaving Ligand in SK-MEL-5 Cell Line.....	37
3.3.5. Effects of Leaving Ligand in HT-1197 Cell Line.....	39
3.3.6. Effects of Leaving Ligand in NTERA2 Cell Line.....	40
4. Discussion.....	41
5. Conclusion.....	45
6. Future Direction.....	45
7. References.....	47

LISTS OF FIGURES

	<u>Pages</u>
Figure 1. Structures of platinum coordination complexes.....	2
Figure 2. Structures of the three FDA platinum chemotherapeutics: Cisplatin, Carboplatin, and Oxaliplatin.....	4
Figure 3. DNA adduct formed by A) Cisplatin B) Oxaliplatin.....	7
Figure 4. Potential Protein Transporters.....	8
Figure 4. Cisplatin accumulation in HEK293 and hOCT2-HEK293 cells.....	10
Figure 6. The structure of Pt(en)mal.....	12
Figure 7. Structure of novel platinum compounds.....	13
Figure 8. Structure of tetrazolium MTT salt and formazan.....	17
Figure 9. A 24-well plate after MTT exposure.....	18
Figure 10. Cellular Dose Response to Pt(en)mal in multiple cell lines.....	21
Figure 11. Boxplot representation of Pt(en)mal survival by cell line.....	23
Figure 12. Cellular Dose Response to Pt(en)CBDCA in multiple cell lines.....	25
Figure 13. Boxplot representation of Pt(en)CBDCA survival by cell line.....	26
Figure 14. Cellular Dose Response to Pt(en)Cl ₂ in multiple cell lines.....	27
Figure 15. Boxplot representation of Pt(en)Cl ₂ survival by cell line.....	28
Figure 16. Cellular Dose Response to carboplatin in multiple cell lines.....	30
Figure 17. Boxplot representation of carboplatin survival by cell line.....	31
Figure 18. Effects of leaving ligand in HEK293 cell line.....	34
Figure 19. Effects of leaving ligand in HT-29 cell line.....	35

	<u>Pages</u>
Figure 20. Effects of leaving ligand in A549 cell line.....	37
Figure 21. Effects of leaving ligand in SK-MEL-5 cell line.....	38
Figure 22. Effects of leaving ligand in HT-1197 cell line.....	39
Figure 23. Effects of leaving ligand in NTERA2 cell line.....	41

LIST OF TABLES

	<u>Pages</u>
Table 1. Comparison of IC ₅₀ for each cell-line compound combination.....	32

CELLULAR TOXICITY OF MALONATO(ETHYLENEDIAMINE)PLATINUM(II) IN MODELS OF CANCER

Sidikat Olanrewaju Olajuwon

August 2021

52 Pages

Directed by: Dr. Blairanne Williams, Dr. Kevin Williams, and Dr. Moon-Soo Kim

Department of Chemistry

Western Kentucky University

Platinum(II) compounds including the three FDA approved drugs, cisplatin, carboplatin, and oxaliplatin, are composed of two structural components, a leaving ligand, and a non-leaving ligand, each attached to a central platinum(II) atom. All bifunctional platinum compounds studied have similar mechanisms of initiating cell death. However, their efficacy as chemotherapeutics depends on the tissues in which the cancer originates. No model has explained these tissue-specific efficacies. We hypothesized that the efficacies of these platinum compounds vary due to structural differences in the leaving ligands. To test the influence of the leaving ligand on cellular survival, novel platinum compounds were synthesized, and toxicological profiles were created in cellular models of cancer from various tissues. The novel platinum compounds used here: malonato(ethylenediamine)platinum(II) (Pt(en)mal), 1,1-cyclobutanedicarboxylato(ethylenediamine)platinum(II) (Pt(en)CBDCA), and dichloro(ethylenediamine)platinum(II) (Pt(en)Cl₂). Cellular models were exposed to the toxicants individually in a dose-dependent manner and then 24 hours after exposure, cell viability was examined by MTT (3-(4,5-dimethylthiazol-2-yl)-2,5-diphenyltetrazolium bromide) assay. Based on our data, Pt(en)mal survival response was higher in the A549 (IC₅₀ = 350 μM ± 3.32), HT-29 (IC₅₀ = 300 μM ± 8.77), and HT-1197 (IC₅₀ = 200 μM ± 1.78) cells compared to the MCF7 (IC₅₀ = 80 μM ± 5.38), HEK293 (IC₅₀ = 60 μM ±

11.68), SK-MEL-5 ($IC_{50} = 60 \mu M \pm 4.01$), and NTERA2 ($IC_{50} = 20 \mu M \pm 5.61$) cell lines. Pt(en)CBDCA survival response was higher in the HT-29 ($IC_{50} = 400 \mu M \pm 6.50$), and MCF7 ($IC_{50} = 200 \mu M \pm 0.98$) cells compared to the SK-MEL-5 ($IC_{50} = 100 \mu M \pm 8.08$), A549 ($IC_{50} = 75 \mu M \pm 2.78$), and HEK293 ($IC_{50} = 50 \mu M \pm 5.74$) cell lines. Pt(en)Cl₂ survival response was also higher in the HT-29 ($IC_{50} = 250 \mu M \pm 4.72$), and A549 ($IC_{50} = 200 \mu M \pm 7.70$) compared to the HT-1197 ($IC_{50} = 50 \mu M \pm 4.20$), MCF7 ($IC_{50} = 50 \mu M \pm 1.85$), HEK 293 ($IC_{50} = 40 \mu M$), SK-MEL-5 (IC_{50} between $30 \mu M \pm 13.63$ and $40 \mu M \pm 3.60$) cell line. Given the differences in IC_{50} based on our data, we conclude that leaving ligand structure influences cell survival of platinum(II) compounds.

1. INTRODUCTION

1.1. Platinum Chemotherapy

Platinum-based chemotherapeutics are the most widely prescribed drugs in modern oncology (administered to about 50% of all cancer patients),¹ either alone or in combination with other anticancer drugs and/or radiation therapy. Platinum-based drugs approved by the FDA are used for the treatment of a broad spectrum of specific cancers including testicular, bladder, ovarian, small and non-small cell lung, breast, melanoma, colorectal, head and neck etc.^{1,2} One of the greatest achievements in chemotherapeutics was the discovery of cisplatin for the treatment of metastatic testicular cancer where the survival in 1970 was nearly 5% of young men, whereas at present more than 80% of such cases are cured.³⁻⁵

1.1.1. The Discovery of Cisplatin

The discovery of cisplatin (*cis*-diamminedichloroplatinum(II), cis-DDP)^{1,6} (Figure 1) was pure serendipity. In 1944, cisplatin was first synthesized and named as Peyrone's chloride by an Italian chemist Michele Peyrone.⁷ However, its antiproliferative properties were not discovered until 1965 by a biophysicist Barnett Rosenberg. During the time, Rosenberg and his colleagues aimed to examine whether electrical current has a potential effect in the cell division of bacteria.⁸ Interestingly, they found that when the bacteria *Escherichia coli* were inoculated in a culture medium with ammonium chloride buffer inside a platinum electrode chamber, the bacteria began to elongate and become filamentous compared to its normal rod shape. As their study progresses, the researchers discovered that the platinum chloride, which formed during electrolysis of the platinum electrode was the active agent in the inhibition of the cell division of the bacteria.⁸

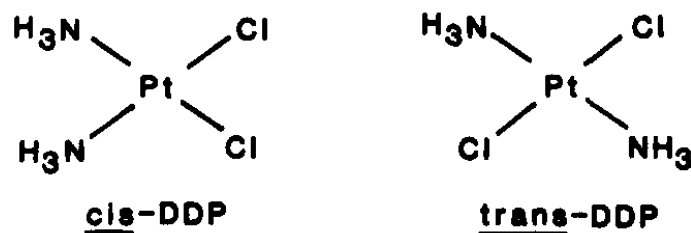


Figure 1. Structures of platinum coordination complexes. Reproduced from Ref. 5.

Rosenberg and his colleagues decided to test series of group 10 transition metals to determine the most effective compound for this inhibition effect. Surprisingly, they all exhibited filamentous growth of the bacteria. The most effective platinum salt, ammonium hexachloroplatinate ((NH₄)₂[PtCl₆]), was found to inhibit cell division of gram-negative bacteria. The *cis* form (Figure 1) of the platinum(IV) complex was reported as the agent responsible for inhibition.^{3,8} Next, they examined the antitumor activity of platinum compounds. Among the platinum compounds tested, only *cis*-platinum(IV)diamminotetrachloride (*cis*-Pt (IV)(NH₃)₂Cl₄) and *cis*-platinum(II)-diamminodichloride (*cis*-Pt (II)(NH₃)₂Cl₂) demonstrated effective inhibition and regression of solid Sarcoma 180 and Leukemia L1210 tumors in Swiss white mice.^{3,9} It was also reported that these platinum compounds were both efficient in successfully regressing large solid tumors in 63% to 100% of the mice, with no resurgence of the tumor after 6 months.⁹

After several years of lab experiments, preclinical research, and clinical trials, *cis*-DDP was approved by the US Food and Drug Administration (FDA) in 1978 as a chemotherapeutic agent and named cisplatin. The clinical success of cisplatin has been

the major motivation for the evolution of the family of platinum compounds, which currently play crucial role in metal-based cancer chemotherapy.¹⁰

1.1.2. FDA Approved Platinum Chemotherapy

Three platinum-based chemotherapeutic agents are currently approved by FDA and used in clinical practice: cisplatin, carboplatin, and oxaliplatin (Figure 2) for the treatment of different cancer types based on the tissue of origin. After the discovery of cisplatin (*cis*-diamminedichloroplatinum(II), *cis*-DDP)¹ as an active antitumor drug mainly for treating testicular cancer, ovarian cancer, and small cell lung cancer, several platinum analogs were subsequently synthesized. Carboplatin (*cis*-diammine(1,1-cyclobutanedicarboxylato)platinum(II)) is a second-generation platinum analog whose chemical structure is similar to that of cisplatin, except that it has a cyclobutanedicarboxylato leaving group (shown in blue) in replace of the two chloride leaving groups of cisplatin (Figure 2). Cisplatin and carboplatin have comparable efficacy in the treatment of small cell lung cancer and ovarian cancer.^{4,10} Carboplatin also possesses similar mechanism of cytotoxic action, mechanism of resistance, and clinical pharmacology as that of cisplatin.^{2,10,11} However, carboplatin exhibits lower reactivity and around 10-fold slower DNA binding kinetics compared to cisplatin.^{2,4,11} Cellular resistance to cisplatin and carboplatin could be due to several factors including reduced platinum uptake, increased platinum efflux, intracellular detoxification by glutathione (GSH), and increased DNA repair.^{4,10} The major mechanism of resistance of these platinum compounds appeared to be reduced platinum uptake,^{10,12} which arises when there's insufficient platinum compound concentration reaching the target DNA. In a study conducted on the role of glutathione in its effectiveness and resistance to platinum

compounds, cisplatin was found to be cross-resistant to carboplatin in both human small cell lung carcinoma and human embryonal carcinoma cell lines.¹³ Additionally, cisplatin cross-resistance to carboplatin was also found in ovarian cancer cell line, which was associated with reduced platinum uptake.¹⁰

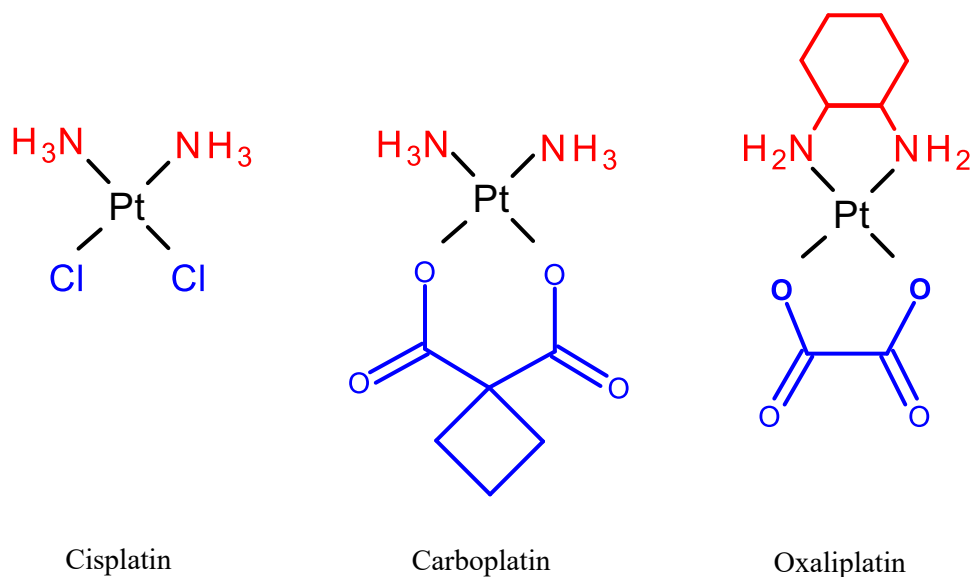


Figure 2. The structures of the three FDA approved platinum chemotherapeutics: cisplatin, carboplatin and oxaliplatin. Platinum(II) compounds are composed of two structural components; the leaving ligands (shown in Red) and the non-leaving ligands (shown in Blue) each attached to a central platinum(II) atom.

Oxaliplatin ((trans-R,R-1,2-diaminocyclohexane)oxalate platinum(II)) is the third-generation platinum analog whose chemical structure is the most distinct (Figure 2). It is the R,R-isomer of a diaminocyclohexane (DACH) platinum(II) compound containing an oxalate leaving group. The DACH non-leaving ligand is more lipophilic, thereby increases the passive uptake of oxaliplatin compared to cisplatin and carboplatin.¹⁴ Similar to cisplatin, oxaliplatin is detoxified by glutathione (GSH)-related

enzymes.¹⁰ Unlike cisplatin and carboplatin, oxaliplatin is mainly effective in the treatment of colon and colorectal cancer.^{10,11} However, the chemotherapeutic use of these platinum-based drugs has been limited by numerous side effects including nephrotoxicity (toxicity of the kidney), ototoxicity (hearing loss), gastrointestinal, neuromuscular symptoms, and drug-resistance of tumor cell.^{1,2,10}

Platinum(II) compounds including these three FDA approved drugs possess similar structural components: a central platinum(II) atom, two leaving ligands and two non-leaving ligands (Figure 2). When platinum(II) compounds are in aqueous solution, the leaving ligands dissociate from the central platinum(II) atom, allowing binding to a biological target DNA. On the other hand, the non-leaving ligands remain attached to the central platinum(II) atom. All platinum(II) compounds studied to date have similar mechanisms of initiating cell death. However, their efficacy as chemotherapeutics depends on the tissues in which the cancer originates. Cisplatin in particular is effective in the treatment of testicular cancer, with more than 95% patient's survival.¹⁵ In contrast, carboplatin has limited efficacy in the treatment of testicular cancer.⁵

1.2. Mechanism of Platinum-Initiated Cell Deaths

Increasing evidence indicates that the cellular target of platinum complexes is primarily the DNA, and their antitumor effects is as a result of their ability to form different types of adducts with the DNA, which inhibits replication and transcription and further induce cell death.^{1,2,14}

1.2.1. Formation of Platinum-DNA Adduct

Despite structural differences, most bifunctional complexes form similar DNA adducts (Figure 3A and 3B).¹⁰ As platinum complexes enter into the cells, the leaving

ligands dissociates from the central platinum atom and slowly undergoes hydrolysis to form chemically reactive aqua (water) species. The activated aqua platinum species thereby allows covalent binding to the target DNA at the nitrogen N7 position of the imidazole ring of purine nucleotide bases (guanine (G) or adenine (A)) to form cross-linking complexes known as the intrastrand adducts and interstrand adducts (Figure 3).^{1,2,10,16} The intrastrand crosslink occurs when platinum-DNA adduct is formed either with two guanines (G) on the same strand of DNA or with guanine (G) and adenine (A) on the same strand of DNA. On the other hand, the interstrand crosslink occurs when platinum-DNA adduct is formed with two guanines (G) on opposite strands of DNA.

The formation of crosslinks causes a bend in the DNA helix which hinders the action of the DNA polymerase (whose main function is to synthesis DNA from deoxyribonucleotides, the building blocks of DNA).^{2,4,10} Thus, leading to defective DNA templates and subsequent blockage of DNA synthesis and replication, which can further lead to cell cycle arrest. The cell's inability to repair the damaged DNA triggers apoptosis (programmed cell death) via p53 intracellular response.¹

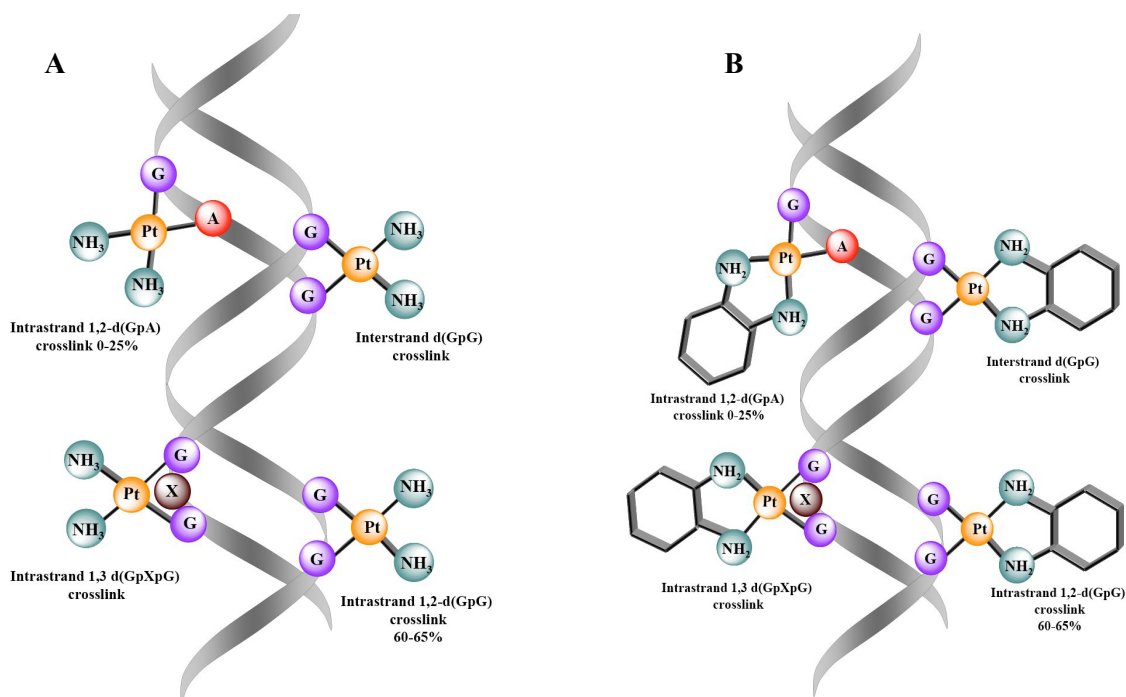


Figure 3. DNA Adducts formed by A) Cisplatin and B) Oxaliplatin. Platinum (II) compounds can interact with DNA to form intrastrand crosslinks (1,2-d(GpA), 1,2-d(GpG), and 1,3-d(GpXpG)), and interstrand crosslink (d(G-G)). Reproduced from Ref. 10.

1.2.2. Accumulation of Platinum by Membrane Transporters

Platinum accumulation is controlled by two main factors: uptake and efflux (Figure 4).¹² Uptake can be referred to as the transport of molecules into the cell while efflux is the transport of molecules out of the cell. The mechanism of cellular uptake and efflux of platinum-based compounds are still not well understood. However, the uptake and efflux of platinum-based compounds are mediated by different transporters. The route of platinum-based drugs uptake in the cells was believed to be mainly by passive diffusion.¹⁷ However, recent studies suggested that platinum-based drugs can also be transported either through transporter-mediated or facilitated diffusion.^{17,18} In contrast to passive diffusion that involves the diffusion of molecules (such as cisplatin) down its concentration gradient, from areas of higher concentration to areas of lower concentration

across a membrane, in facilitated diffusion, molecules diffuse across the plasma membrane via the help of membrane proteins, such as carriers and channel proteins (Figure 4).¹⁹

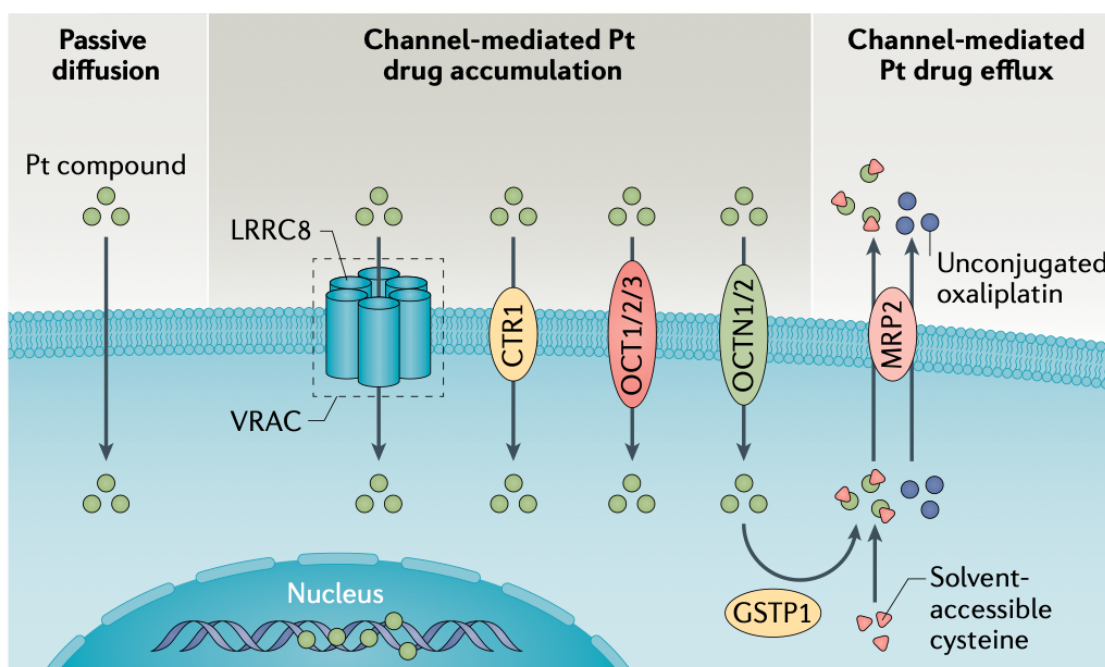


Figure 4. Potential platinum transporters. Reproduced from Ref. 12.

Carrier proteins such as copper transporter receptor-1 (CTR1), organic cation transporters (OCT1, OCT2, and OCT3), organic cation/carnitine transporters (OCTN1, and OCTN2), and multidrug resistance-associated protein 2 (MRP2); and channel proteins such as the volume-regulated anion channels (VRAC) have been proposed to transport platinum in and out of the cell (Figure 4).¹² VRAC is composed of the leucine-rich repeat-containing 8 (LRRRC8) subunits (Figure 4). VRAC plays a dual role in cellular platinum response, as it mediates cisplatin uptake and facilitates apoptosis (programmed

cell death). Under isotonic condition, nearly 50% of cisplatin uptake was dependent on LRRC8A and LRRC8D subunits of VRAC.²⁰ Intriguingly, the loss of LRRC8A and LRRC8D subunits was found to increase resistance of clinical cisplatin or carboplatin concentrations.^{12,20} There is also an extensive evidence that the conjugation of cisplatin with glutathione might be catalyzed by glutathione-S-transferase pi 1 (GSTP1), which mediates the binding of platinum-based drugs to free cysteines and subsequent efflux from the cells via MRP2 (Figure 4).^{11,12,21} Furthermore, MRP2 was indicated to export unconjugated oxaliplatin out of the cell (Figure 4).¹²

1.2.2.1. Cellular Uptake of Platinum

Focusing on cisplatin, studies have shown that the cellular uptake of cisplatin is mediated primarily by the organic cation transporter 2 (OCT2) and copper transporter receptor-1 (CTR1). Three isoforms of OCTs (OCT1, OCT2, and OCT3) have been recognized in humans.²² OCT2 is mainly expressed in the kidney and has been suggested to be the major transporter for cisplatin uptake. Also, in excretory organs such as the kidney, OCT2 are highly expressed when the proximal tubules are damaged by antitumor therapy with platinum derivatives.²¹ Hence, OCT2 can be a target for renoprotection.

In a study, it was demonstrated that cisplatin uptake was increased by OCT2 overexpression in human embryonic kidney293 (HEK293) cells (Figure 5).²³ In the study, the isoforms hOCT1 and hOCT2 demonstrated how cisplatin interacts with hOCT2, and not with hOCT1. Since hOCT2 is present in human hepatic cells,²⁴ this finding best explains the organ-specific toxicity of cisplatin with toxic effects in kidney (Figure 5). Carboplatin and oxaliplatin showed less nephrotoxic counterpart of cisplatin, and there was no interaction with hOCT2.²³ It could be that these compounds cannot

freely penetrate through the proximal tubular cells, because of their inability to interact with hOCT2 and therefore are less toxic for the renal tubular cells.

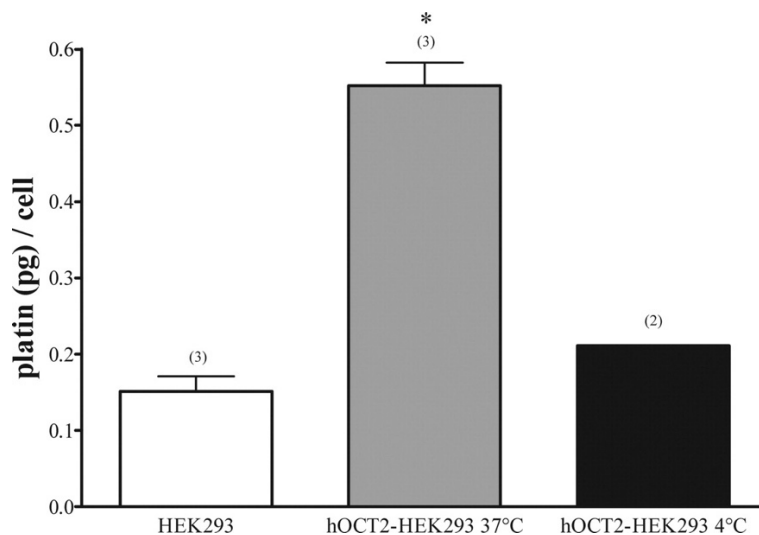


Figure 5. Cisplatin accumulation in HEK293 (white column) and hOCT2-HEK293 (gray column) cells after 10 minutes incubation with 100 $\mu\text{mol/L}$ cisplatin. Experiments performed with hOCT2-HEK293 cells at 4°C are also shown (black column). Values are mean \pm SEM expressed as pg cisplatin per cell. * Statistically significant effect (analysis of variance, $P < 0.05$). Above the columns are the number of observations. Reproduced from Ref 23.

CTR1, which is expressed in the proximal tubular cells of adult kidney and cardiac tissue, was also suggested to play a key role in cisplatin uptake. In *in vitro* studies, it was reported that the downregulation of CTR1 significantly reduced cisplatin uptake and cytotoxicity.^{5,25,26} These two membrane transporters (OCT2 and CTR1) work together simultaneously, which results in disproportionate distribution of cisplatin in the body.²⁷ It was also shown that OCT1 and OCT2 markedly increased cellular uptake and cytotoxicity of oxaliplatin in six transfected colon cancer cell lines, but such effects were

not observed in cisplatin or carboplatin, indicating that oxaliplatin is an excellent substrate of these transporters.²⁸

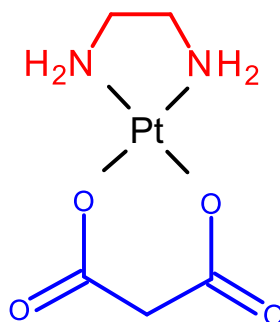
1.2.2.2. Cellular Efflux of Platinum

Studies have shown that the efflux of cisplatin from renal tubular epithelial cells is mediated by MATE1 transporter. Multidrug and toxin extrusion 1 (MATE1) are expressed in the membrane of the renal proximal tubules.¹⁹ In an *in vitro* experiment conducted by Nakamura et al., cells transfected with MATE1 showed increased cellular uptake of cisplatin compared to the control.²⁹ It has also been reported in both *in vivo* and *in vitro* that the genetic deletion of MATE1 in a mice model makes them more susceptible to cisplatin nephrotoxicity.^{21,29}

Earlier studies have reported partial role for efflux proteins such as the multidrug resistance-associated proteins (MPR1, MPR2, MPR3, MPR4, and MPR5) in mediating platinum-based drugs efflux.¹¹ However, recent studies have shown the P-type copper-transporting ATPases (ATP7A and ATP7B) to involve in cellular cisplatin efflux.¹² For example, in a study where human ovarian carcinoma cells were transfected with ATP7A, data showed only 1.5 fold increase in ATP7A expression but was sufficient to render the cells resistant to cisplatin, carboplatin, and oxaliplatin.³³ These transporters play crucial role in the cellular copper levels in order to help prevent high accumulation of intracellular copper concentrations which are toxic to the cells.^{1,10,12} ATP7A is mainly expressed in endothelial cells, intestine, and vascular smooth muscle while ATP7B is mainly expressed in the liver and the brain. ATP7A and ATP7B mediates cisplatin efflux from the cell.²¹ Aside cisplatin, these transporters also interact with carboplatin and oxaliplatin.

1.3. Novel Platinum Compounds

Using a novel platinum(II) compound, Pt(en)mal (malonato(ethylenediamine)-platinum(II)), we will examine the effects of the chemical structure on cytotoxicity using various cellular models of human cancer. Pt(en)mal compound is similar in structure to the FDA approved platinum drugs especially carboplatin. In carboplatin, the non-leaving ligand, consists of two amines attached to the central platinum atom (Figure 2). Similarly, in our novel compound, two nitrogen atoms are attached to the central platinum atom, but there is a two-carbon bridge (ethylene) between them forming a closed ring (Figure 6).



Pt(en)mal

Figure 6. The structure of Pt(en)mal (malonato-(ethylenediamine)platinum (II)). Red denotes non-leaving ligands while blue denotes leaving ligands.

Additional novel platinum(II) compounds used in this study includes Pt(en)Cl₂ (dichloro(ethylenediamine)platinum(II)), and Pt(en)CBDCA (1,1-cyclobutanedicarboxylato(ethylenediamine)platinum(II)). Both platinum compounds have the same non-leaving ligand, ethylenediamine (en) as Pt(en)mal, varying only at the leaving ligand as shown in Figure 6. Pt(en)CBDCA is structurally similar to carboplatin

as they share same cyclobutanedicarboxylate leaving ligand whereas, Pt(en)Cl₂ share similar dichloride leaving ligand structure to cisplatin (Figure 2 and 7). This study uses these novel platinum analogues to explore leaving ligand effects on cell type toxicity.

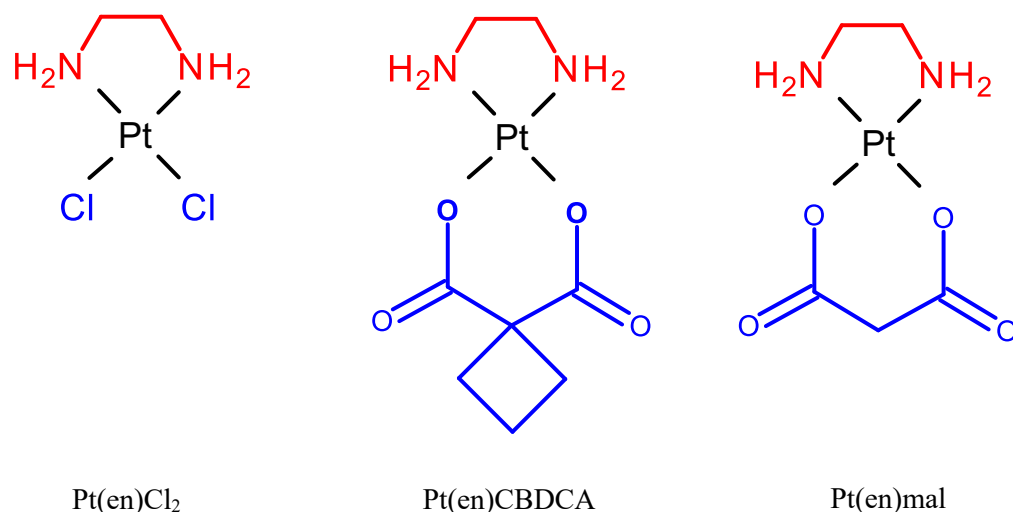


Figure 7. Structure of Novel Platinum Compounds. Each compound has similar ethylenediamine (en) non-leaving ligands (shown in Red) but varying leaving ligand structure (shown in Blue) where Cl₂ = dichloride, CBDCA = cyclobutanedicarboxylate, and mal = malonate.

Though extensive studies have shown that all platinum(II) compounds possess similar mechanism of platinum initiating cell deaths, no clear model has been proposed to explain why platinum(II) compounds target different tissues of cancer origin. We hypothesized that the cell survival response of these platinum compounds varies due to structural differences in the leaving ligands. To test this hypothesis, cell survival will be examined after exposure to increasing concentrations of each platinum compound. We will also compare the effects of the leaving ligand structure among our three novel

platinum compounds (Pt(en)mal, Pt(en)CBDCA, and Pt(en)Cl₂) on cellular response in specific cell types.

2. MATERIALS AND METHODS

2.1. Cell Culture and Reagents

For the purpose of this study, seven different cell lines were used including the non-cancerous human embryonic kidney (HEK293, CRL-1573), small cell lung carcinoma (A549, CCL-185), colorectal adenocarcinoma (HT-29, HTB-38), melanoma (SK-MEL-5, HTB-70), urinary bladder carcinoma (HT-1197, CRL-1473), human testicular embryonic carcinoma (NTERA2, CRL-1973), and human breast adenocarcinoma (MCF7, HTB-22). The HEK293 cells were generated by transforming primary human embryonic kidney with adenovirus 5 DNA which regulates the cell cycle that enables the cells to continuously grow.⁴ HEK293 cells was believed to be derived from embryonic kidney cells. However, prediction has arisen that the cells might not actually be kidney cells, but neuronal in origin. Nevertheless, the HEK293 cell line was chosen as our control cell line because it's well studied, and we understand what the mutation is to allow it grow on the culture dish. In other words, we understand the variant in it compared to these other cell lines that were cultured from human samples where there could be multiple mutation. These cell lines were purchased from American Type Culture Collection (ATCC, Manassas, VA, USA) and cultured in appropriate medium nutrients, supplemented with 10% fetal bovine serum (FBS, Cat. #SH30396.03, HyClone), and 1% penicillin-streptomycin solution (Cat. #P0781, Sigma-Aldrich) at 37°C in a humidified 5% CO₂ Galaxy 170 S incubator. Dulbecco's modified Eagle's medium (DMEM, Cat. #30-2003, ATCC / Cat. #10-013-CV, Corning) was used for

HEK239 cells and Ntera2 cells; Kaighn's modification of Ham's F-12 (F-12K, Cat. #30-2004, ATCC / Cat. #10-025-CV, Corning) for A549 cells; McCoy's 5A medium (McCoy's 5A, Cat. #30-2007, ATCC / Cat. #SH30200.01, Cytiva) for HT-29 cells; and Eagle's minimum essential medium (EMEM, Cat. #30-2003, ATCC / Cat. #10-009-CV, Corning / Cat. #12-611Q, Lonza) for SK-MEL-5, MCF7, and HT-1197 cells.

The cells were subculture per ATCC recommendation. All work with cells was done in compliance with the Institutional Biosafety Committees guidelines. In the biological safety cabinet (1300 Series A2, Thermo Scientific), after the growth of adherent cells reached 90-95% confluency, cells monolayer was washed once or twice with 37°C phosphate-buffered saline (PBS, Cat. #21-040-CV, Corning) without magnesium and calcium to remove dead cells or any residual FBS that may block the action of trypsin. Then, 1-2 mL of the 37°C digestive enzyme, trypsin (1X, Cat. #1689349, MP Biomedicals LLC) without calcium and magnesium, was added to cover the cell monolayer and incubated at 37°C for 5-15 minutes depending on the cell type. The cells were observed under the microscope to ensure that they are detached from the surface. Once the cells were detached, 4-6 mL of 37°C complete media containing FBS and penicillin-streptomycin solution was added to inhibit further activity of trypsin that could damage the cells. The desired concentration of cell suspension was seeded in new 10 cm tissue culture dish (Cat. #353003, Corning / Cat. #10062-880, VWR) and properly labeled. Fresh complete media was also added to the new tissue culture dish and incubated in a humidified 37°C, 5% CO₂ incubator.

2.2. Platinum Compounds

Our novel platinum compounds including Pt(en)mal (malonato(ethylenediamine)-platinum(II)), and Pt(en)CBDCA (1,1-cyclobutanedicarboxylato(ethylenediamine)-platinum(II)) used for these experiments were synthesized in the laboratory of our collaborator, Dr. Kevin Williams. The FDA approved carboplatin (Cat. #C2043, TCI America), and Pt(en)Cl₂ (dichloro (ethylenediamine) platinum (II), Cat. # 244929, Alfa Asar) were commercially available. For MTT assays (described in section below), 1mM stock solution of each platinum compound were prepared by dissolving them in appropriate medium based on the cell type. The 1mM stock solution are refrigerated and used up within two weeks.

2.3. Cell Growth Curves

Growth curves were carried out periodically to assess the cell viability, proliferation of each cell lines, and determine the number of cells to use for assays. Four concentrations of each cell lines were chosen (ranging from 400,000 - 750,000 cells per plate) and were evenly plated in three separate 24-well plates (that is, a total of 18 wells per concentration). Each plate was read at t=24 hours, t=48 hours, and t=72 hours incubation period respectively to determine the time-dependent increase in cell number. These time differences were chosen to examine the proliferation of the cells at various time intervals. The colorimetry MTT assay (as described in MTT assay section below) was used to measure mitochondrial activity from which the number of living cells is inferred. Absorbance values were plotted against each concentration at time (t) to determine the most appropriate concentration of cells to use for assays, which is ideally where the cells are in the logarithmic (Log) growth phase. In the Log phase, the cells are at their highest growth. Each cell line often establishes different cell growth during this

phase. Based on the growth curve analysis, the concentrations chosen for each cell line includes A549, HT-29, and SK-MEL-5: 550,000 per 24-well plate; HEK293, NTERA2, and MCF7: 650,000 cells per 24-well plate; and HT-1197: 750,000 cells per 24-well plate.

2.4. MTT Assay

Cell viability in response to increasing concentrations of each individual platinum(II) compound was evaluated in 24-well (Corning, USA) flat-bottomed cell culture plates by using the standard MTT (3-[4,5-dimethylthiazole-2-yl]-2,5-diphenyl-tetrazolium bromide)³⁴ colorimetric assay (Figure 8). The assay measures cellular metabolic activity as a proxy for cell viability. Viable cells contain NADPH-dependent oxidoreductase enzymes (a mitochondrial reductase enzymes) which reduces the yellow MTT salt to an insoluble purple formazan.³⁵ Insoluble formazan is then dissolved in dimethyl sulfoxide (DMSO) and Sorenson's buffer (0.1M glycine, 0.1M sodium chloride, pH 10.5) to produce a purple-colored cell lysate (Figure 9). The absorbance of the colored solution can be quantified at specific wavelength using a spectrophotometer/plate reader. The darker the purple-colored solution, the higher the number of viable active cells.

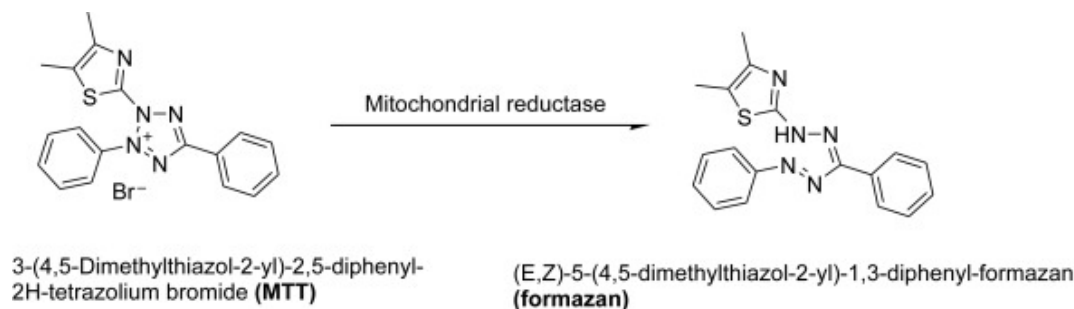


Figure 8. Structure of tetrazolium MTT salt and formazan. The yellow MTT salt are reduced to formazan by the mitochondrial reductase enzyme. Reproduced from Ref. 35.



Figure 9. A 24-well plate after MTT exposure. Darker purple color of solution denotes more cell survival.

At the start of each experiment ($t=0$), the stock plates of an individual cell type were subcultured at 90-95% confluency and counted using a hemocytometer and the Corning CytoSmart cell counter (Cat. #6749, Corning). The cells were then plated between the concentration of 23,000 to 31,250 cells per well (dependent on growth curve analysis) across a 24-well plate with the aid of an Eppendorf repeater pipette. After overnight incubation ($t=24$ hours), the medium was aspirated, and the cells were exposed to increasing concentration of platinum compounds in triplicate. Media only was used as the untreated control. The plate was then incubated for another 24 hours. At least three replicate experiments ($n=3$) were completed for each cell line-to-compound combination. After 24 hours incubation ($t=48$ hours), the platinum compound was aspirated from the plate, and 10% MTT salt (3-[4,5-dimethylthiazole-2-yl]-2,5-diphenyl-tetrazolium bromide, Across Organics) solution was then introduced ($500 \mu\text{L}$) to each well and incubated further for 3.5 hours. The MTT in media solution was prepared by diluting a stock solution of MTT (5 mg / 1 mL in phosphate-buffered saline (PBS)) and adding the

appropriate nutrient medium to a final concentration of 10% MTT to media in a 50 mL conical tube.

After the 3.5 hours incubation period, the MTT solution was aspirated and then treated with the solubilizing solution (DMSO and Sorenson's buffer) to lyse the cells and solubilize the formazan salt. The absorbance values of the colored solution were then read at 550 nm wavelength using the BioTek Synergy HTX multi-mode plate reader. The triplicate values for each concentration were normalized to the average of the three untreated control wells to establish 100 percent (%) cell survival, and the background absorbance were also subtracted. Specifically, we assumed that the untreated control wells were at 100% survival and correlated the treated wells absorbance values to that of the untreated control wells absorbance values. The background absorbance value was obtained by evenly plating 500 μ M of 10% MTT in media in six wells of a 24 well plate, then incubated for 3.5 hours, and read absorbance at 550 nm wavelength.

2.5. Statistical Analysis

A full statistical analysis (multiple linear regression model, and pairwise multiple comparisons using t-tests) on Pt(en)mal cellular response was completed by the Kentucky INBRE core, at the University of Kentucky. I completed additional statistical analysis including Pt(en)CBDCA cellular response, Pt(en)Cl₂ cellular response, and the effects of leaving ligands in specific cell types. Multiple linear regression model and t-test analysis on IBM SPSS Statistics 26 software was used to calculate the statistical significance using all experimental values. Data are presented as mean of at least three independent experiments (n=3) \pm standard error (S.E).

3. RESULTS

3.1. Platinum Cellular Response

To determine the cell survival response to the novel platinum(II) compounds, individual cancer cell lines were exposed to increasing concentrations of each compound. MTT assays were completed to determine cell response after exposure to each of the novel compounds and the FDA-approved chemotherapeutic carboplatin. Carboplatin was replicated as a control thereby, allowing for direct comparison to the other platinum compounds.

3.1.1. Pt(en)mal Cellular Response

In the Pt(en)mal (Figure 6), MTT assays to assess cell viability were carried out on seven different cellular models of human cancer HEK293, HT-29, SK-MEL-5, A549, MCF7, NTERA2, and HT-1197. Each cell line was exposed to increasing concentrations of the platinum compound in triplicate for each experiment (where n = an individual experiment) thereby, generating a dose dependent survival curve for each compound. As illustrated in Figure 10, the cell lines were designated with different color. For the cancerous cell lines: HT-29 (pink) represents the colorectal adenocarcinoma cell line, SK-MEL-5 (orange) represents the melanoma cell line, A549 (aqua blue) represents the small cell lung carcinoma cell line, MCF7 (royal blue) represents the human breast adenocarcinoma cell line, NTERA2 (green) represents the human testicular embryonic carcinoma cell line, and HT-1197 (red) represents the urinary bladder carcinoma cell line. These designated cell line colors will remain same for all figures.

Cellular Dose Response to Pt(en)mal in Multiple Cell Lines

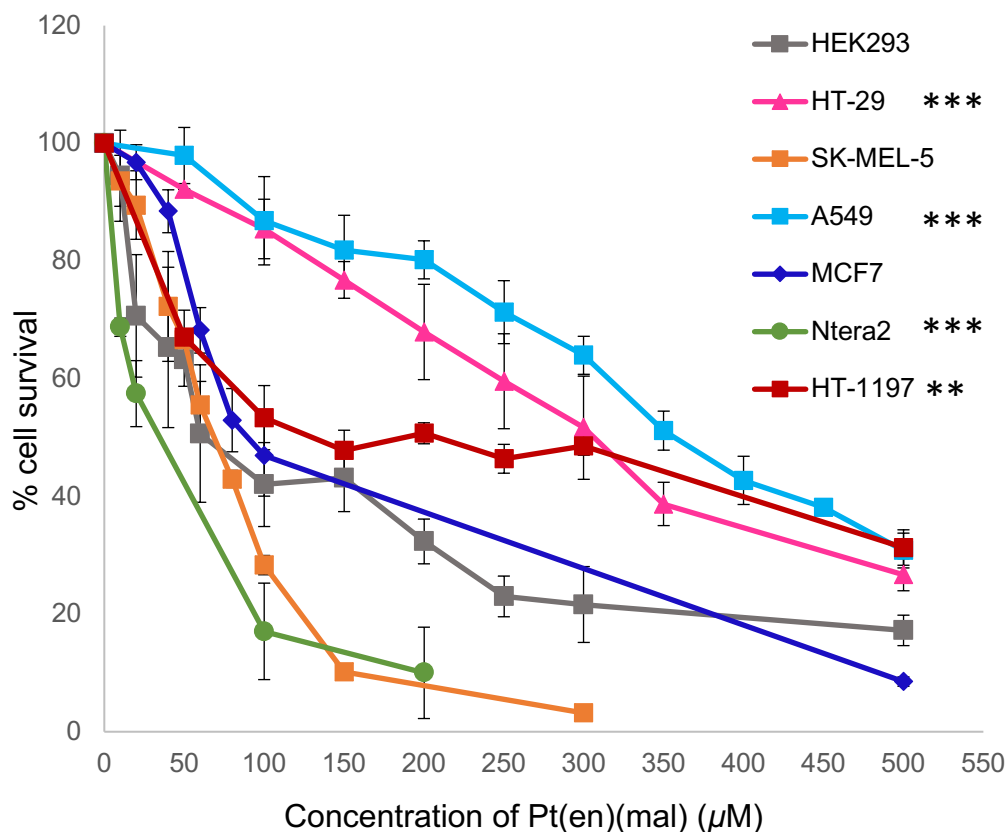


Figure 10. Cellular Dose Response to Pt(en)mal in Multiple Cell Lines. 750,000 cells were plated for HT-1197 (red); 650,000 cells were plated for HEK293 (grey), HT-29 (pink), Ntera2 (army green), and MCF7 (royal blue); 550,000 cells were plated for A549 (aqua blue), and SK-MEL-5 (burnt orange) per 24-well plate. For each experiment (n, ± standard error (s.e.)), equal numbers of cells were exposed to increasing concentrations of Pt(en)mal in triplicate for 24 hours. Values are normalized percent cell survival of HT-1197 (n=3), HEK293 (n=8), HT-29 (n=5), NTERA2 (n=6), MCF7 (n=4), A549 (n=13), and SK-MEL-5 (n=4) in response to varying concentrations of Pt(en)mal. * Represents statistically significant cellular responses in HT-29, SK-MEL-5, A549, MCF7, Ntera2, and HT-1197 cells compared to control HEK293 cells as shown close to their label on the graph (multiple linear regression analysis, * p < 0.05,

The resulting data created a toxicity profile of Pt(en)mal in the multiple cell lines (Figure 10). Using the average absorbance of the three untreated control wells (0 μ M concentration of Pt(en)mal) for each cell types, the percent cell survival was established as 100% by normalization (Figure 10). In other words, the absorbance values from the three individual wells were averaged for each concentration, background absorbance was subtracted from averages, then normalized to the average of the three untreated control wells. At increasing concentrations of Pt(en)mal for each cell line, there was a decrease in survival. The toxicity level of the platinum compound varied by cell line as indicated by the inhibitory concentration at 50% survival (IC_{50}). Usually, the IC_{50} helps determine the toxicity of the compound. For the A549 and HT-29 cell lines, cell survival was greater even at increased concentrations of the compound compared to the other cell lines. Additionally, the survival plateau around 30% cell survival at 500 μ M concentration of Pt(en)mal (Figure 10). In contrary, the NTERA2 and SK-MEL-5 cells lines displayed a decreased cell survival even at concentrations of 100 μ M and below compared to the other cell lines.

Comparing the inhibitory concentration at 50% survival (IC_{50}) between each cell line, it also indicated that each cell line has a unique response to Pt(en)mal (Table 1). The small cell lung carcinoma (A549, p-value < $2e^{-16}$), colorectal adenocarcinoma (HT-29, p-value = $1.41e^{-13}$), and urinary bladder carcinoma (HT-1197, p-value = 0.00508) cell lines showed significant increase in cell survival to the compound compared to the non-cancerous control HEK293 cell line (Figure 10). However, the human testicular embryonic carcinoma (NTERA2, p-value = $1.02e^{-10}$) cell line showed a significant decrease in their survival after exposure to the Pt(en)mal compared to the non-cancerous

control HEK293 cell line (Figure 10). There was no significant difference in MCF7 and SK-MEL-5 cell survival response when compared to the non-cancerous HEK293 cell line. As observed in the re-graphed data represented with boxplots (Figure 11), there was a cell line effect for Pt(en)mal. The normalized survival decreased at a different cell-type dependent manner. In particular, NTERA2 cells appeared to have a much lower survival after exposure to Pt(en)mal compared to the other cell lines (Figure 11). Toxicity increased for the NTERA2 model with a plateau in survival below 20% cell survival at 100 μ M concentration (Figure 10).

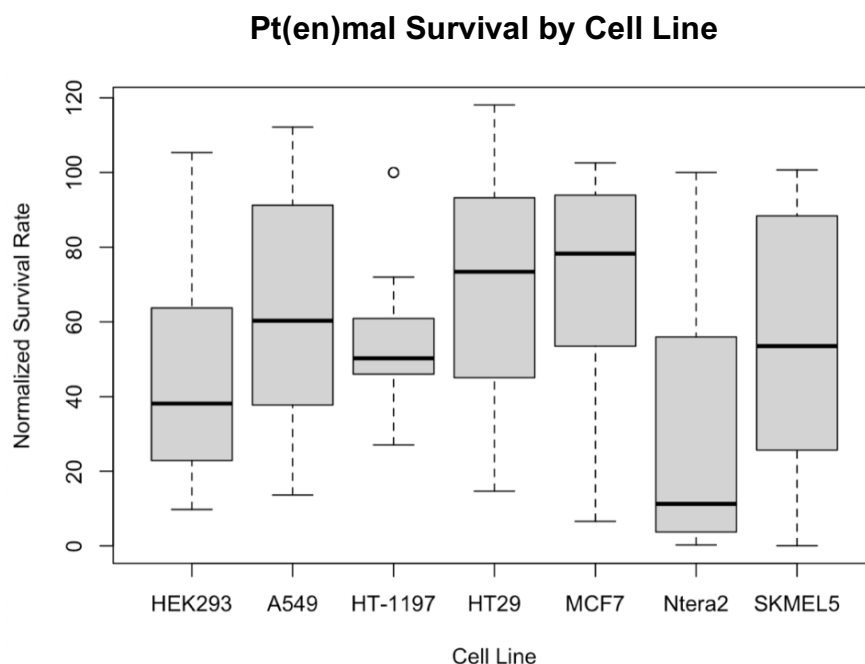


Figure 11. Boxplot representation of normalized survival by cell line when exposed to varying concentration of Pt(en)mal. 750,000 cells were plated for HT-1197; 650,000 cells were plated for HEK293, HT-29, NTERA2, and MCF7; 550,000 cells were plated for A549, and SK-MEL-5 per 24-well plate. For each experiment (n, \pm s.e.), equal numbers of cells were exposed to increasing concentrations of Pt(en)mal in triplicate for 24 hours. Values are normalized percent cell survival of HT-1197 ($n=3$), HEK293 ($n=8$), HT-29 ($n=5$), NTERA2 ($n=6$), MCF7 ($n=4$), A549 ($n=13$), and SK-MEL-5 ($n=4$) in response to varying concentrations of Pt(en)mal. The normalized survival rate decreased at different rate depending on the cell line.

3.1.2. Pt(en)CBDCA Cellular Response

Pt(en)CBDCA has similar ethylenediamine (en) non-leaving ligand structure to Pt(en)mal. Additionally, Pt(en)mal have closely similar leaving ligand structure to Pt(en)CBDCA except the lack of cyclobutane attached (Figure 7). To explore leaving ligand effects on cell toxicity, Pt(en)CBDCA was also tested on cellular models of cancer. Here, MTT assay was performed on five different cell lines: HEK293, HT-29, SK-MEL-5, A549,³⁶ and MCF7. Using the MTT data, a toxicity profile was established for Pt(en)CBDCA in multiple cell lines (Figure 12). The survival responses of each cell line were normalized to the untreated control wells (0 μ M concentration of Pt(en)CBDCA) to establish 100% percent cell survival. Cell survival decreased as concentration increases as seen with the other platinum compounds. For example, initially at 0 μ M concentration of Pt(en)CBDCA (no treatment), the percent cell survival of A549 (aqua blue) was established as 100% by normalization, the half-maximum inhibitory concentration at 50% survival (IC_{50}) was within $75 \mu\text{M} \pm 2.78$ (Table 1), and it plateau around 40% cell survival at 300 μ M concentration (Figure 12). The IC_{50} values between each cell line also differs (Table 1), which is an evidence that each cell line responds to Pt(en)CBDCA differently.

The data showed a cell line effect for this compound as with the other tested compounds. In the re-graphed data represented by boxplots in Figure 13, the normalized survival decreased differently based on the cell type. For instance, the melanoma (SK-MEL-5) cell line appeared to have a decreased survival compared to the other cell lines. There was an increase in toxicity at higher concentrations in the SK-MEL-5 but survival plateaus below 20% cell survival at 200 μ M concentration (Figure 12). The HT-29 (pink)

and MCF7 (royal blue) cell lines showed a significant increase in survival compared to the non-cancerous control HEK293 cell line (Figure 12) after exposure to Pt(en)CBDCA. However, there was no significant difference in the A549 (aqua blue) and SK-MEL-5 (orange) survival response to the compound when compared to the control HEK293 (grey) cell line.

Cellular Dose Response to Pt(en)CBDCA in Multiple Cell Lines

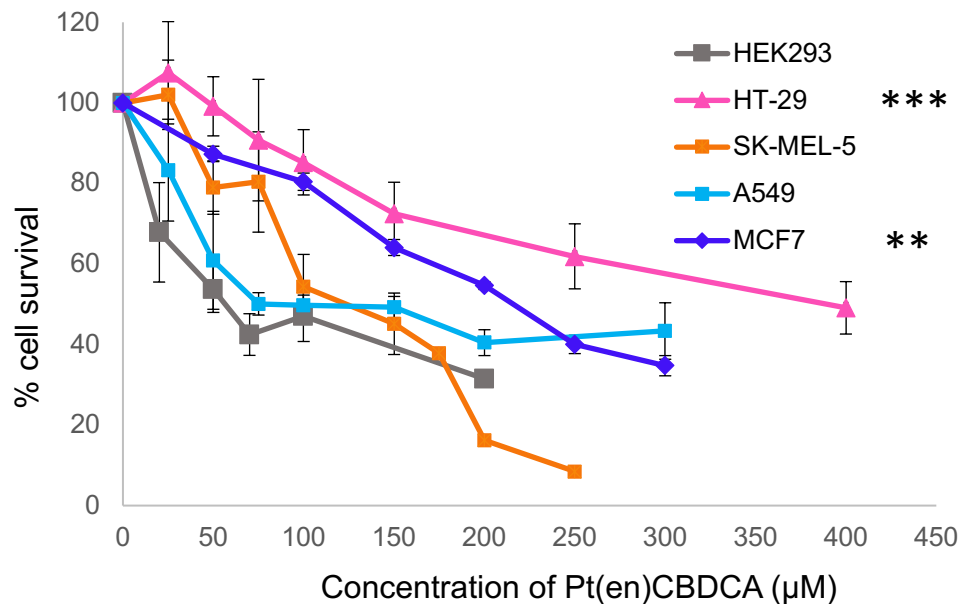


Figure 12. Cellular Dose Response to Pt(en)CBDCA in Multiple Cell Lines. 750,000-650,000 cells were plated for MCF7 (royal blue); 650,000 cells were plated for HEK293 (grey), HT-29 (pink), and SK-MEL-5 (burnt orange); 550,000-600,000 cells were plated for A549 (aqua blue) per 24-well plate. For each experiment (n , \pm standard error (s.e.)), equal numbers of cells were exposed to increasing concentrations of Pt(en)CBDCA in triplicate for 24 hours. Values are normalized percent cell survival of MCF7 ($n=3$), HEK293 ($n=8$), HT-29 ($n=7$), SK-MEL-5 ($n=8$), and A549 ($n=4$) in response to varying concentrations of Pt(en)CBDCA. * Represents statistically significant cellular responses in HT-29, SK-MEL-5, A549, and MCF7 cells compared to control HEK293 cells as shown close to their label on the graph (multiple linear regression analysis, ** $p < 0.01$, *** $p < 0.001$).

Pt(en)CBDCA Survival by Cell Line

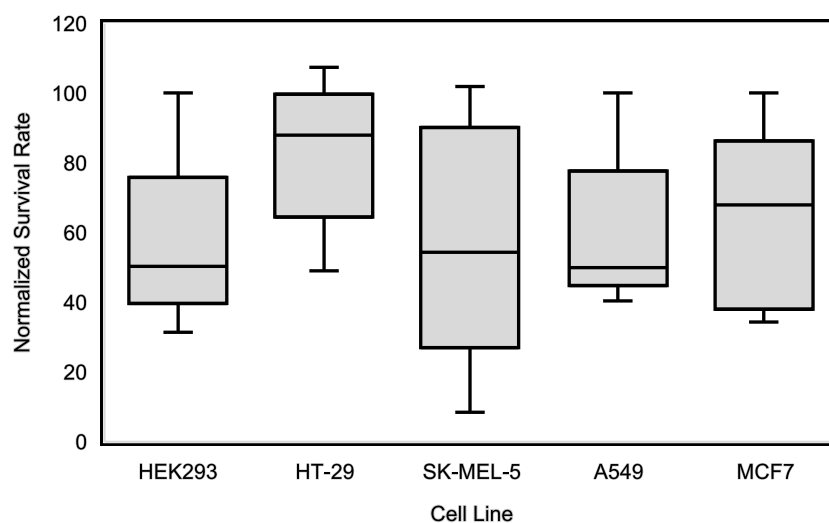


Figure 13. Boxplot representation of normalized survival rate by cell line when exposed to varying concentration of Pt(en)CBDCA. 750,000-650,000 cells were plated for MCF7; 650,000 cells were plated for HEK293, HT-29, and SK-MEL-5; 550,000-600,000 cells were plated for A549 per 24-well plate. For each experiment (n, \pm s.e.), equal numbers of cells were exposed to increasing concentrations of Pt(en)CBDCA in triplicate for 24 hours. Values are normalized percent cell survival of MCF7 ($n=3$), HEK293 ($n=8$), HT-29 ($n=7$), SK-MEL-5 ($n=8$), and A549 ($n=4$) in response to varying concentrations of Pt(en)CBDCA. The normalized survival rate decreased at different rate depending on the cell line.

3.1.3. Pt(en)Cl₂ Cellular Response

For the Pt(en)Cl₂, tetrazolium MTT assay was conducted on seven different cell lines: HEK293, HT-29, SK-MEL-5, A549, MCF7, NTERA2, and HT-1197 to determine their survival response to the compound. The resulting data created a toxicity profile of Pt(en)Cl₂ in multiple cell lines as shown in Figure 14. The survival responses of each cell line were normalized to the untreated control wells (0 μ M concentration of Pt(en)Cl₂) to establish 100% percent cell survival. Data from the NTERA2 (green), HEK293 (grey),

SK-MEL-5 (orange), and MCF7 (royal blue) cell lines showed lower survival at increased concentrations as they plateau below 20% survival compared to the other cell lines (Figure 14).

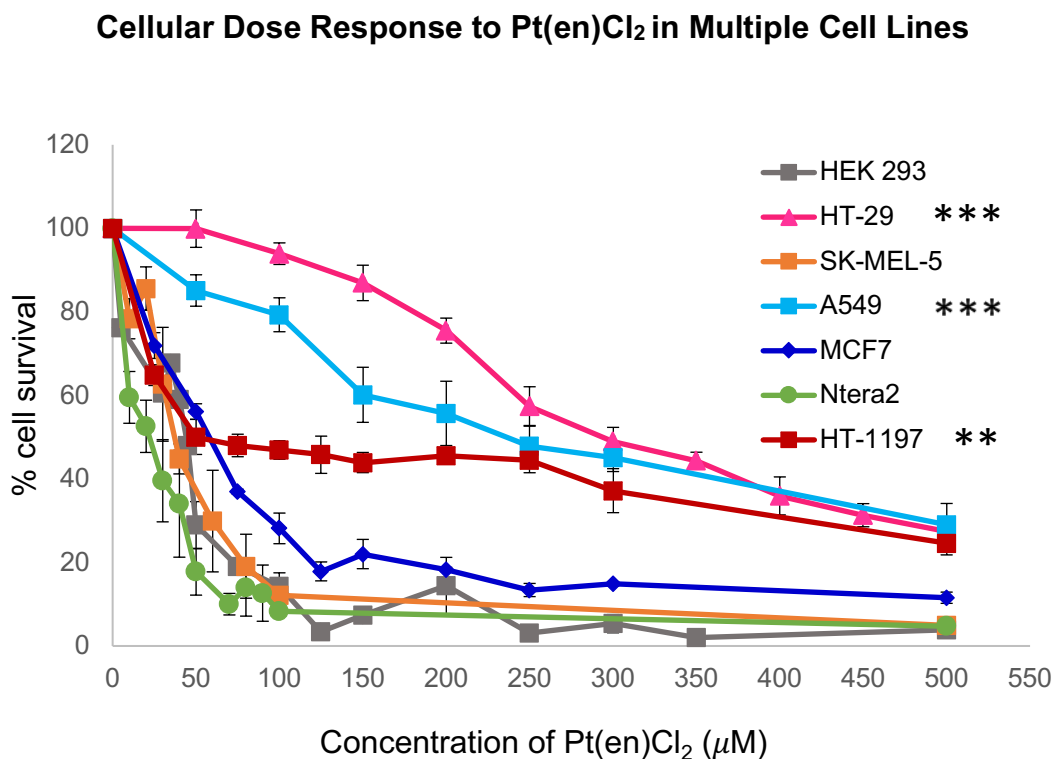


Figure 14. Cellular Dose Response to Pt(en)Cl₂ in Multiple Cell Lines. 750,000 cells were plated for HT-1197 (red); 650,000 cells were plated for HEK293 (grey), HT-29 (pink), A549 (aqua blue), NTERA2 (green), and MCF7 (royal blue); 550,000 cells were plated for SK-MEL-5 (orange) per 24-well plate. For each experiment (n, ± standard error (s.e.)), equal numbers of cells were exposed to increasing concentrations of Pt(en)Cl₂ in triplicate for 24 hours. Values are normalized percent cell survival of HT-1197 (n=6), HEK293 (n=5), HT-29 (n=5), A549 (n=4), NTERA2 (n=5), MCF7 (n=5), and SK-MEL-5 (n=3) in response to varying concentrations of Pt(en)Cl₂. * Represents statistically significant cellular responses in HT-29, SK-MEL-5, A549, MCF7, Ntera2, and HT-1197 cells compared to control HEK293 cells as shown close to their label on the graph (multiple linear regression analysis, ** p < 0.01, *** p < 0.001).

Pt(en)Cl₂ Survival by Cell Line

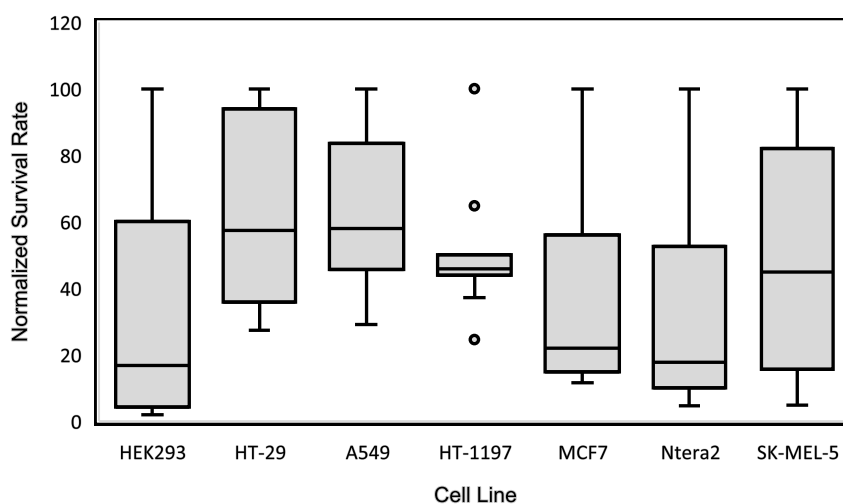


Figure 15. Boxplot representation of normalized survival rate by cell line when exposed to varying concentration of Pt(en)Cl₂. 750,000 cells were plated for HT-1197; 650,000 cells were plated for HEK293, HT-29, A549, NTERA2, and MCF7; 550,000 cells were plated for SK-MEL-5 per 24-well plate. For each experiment (n, ± s.e.), equal numbers of cells were exposed to increasing concentrations of Pt(en)Cl₂ in triplicate for 24 hours. Values are normalized percent cell survival of HT-1197 (n=6), HEK293 (n=5), HT-29 (n=5), A549 (n=4), NTERA2 (n=5), MCF7 (n=5), and SK-MEL-5 (n=3) in response to varying concentrations of Pt(en)Cl₂. The normalized survival rate decreased at different rate depending on the cell line.

As observed in the re-graphed data represented by boxplots (Figure 15), there was difference in the normalized survival of each cell line response to Pt(en)Cl₂. Even in the non-cancerous HEK293 cell lines (which serves as a baseline control), their survival was lower compared to the HT-29 cell line (Figure 15). There was a significant increase in survival response in the following cell types: colorectal (HT-29), small cell lung (A549), and urinary bladder (HT-1197) to Pt(en)Cl₂ when compared to the control HEK293 cell line (Figure 14). In contrast, there was no significant difference in survival response

among the melanoma (SK-MEL-5), testicular (NTERA2), and breast (MCF7) models to Pt(en)Cl₂ when compared to the control HEK293 cell line. The IC₅₀ values determined for each cell line also varied for each cell line-Pt(en)Cl₂ combination and showed a cell line effect in the Pt(en)Cl₂ (Table 1).

3.1.4. Carboplatin Cellular Response

Six different cell lines including HEK293, HT-29, SK-MEL-5, A549, MCF7, and HT-1197 were exposed to increased concentrations of carboplatin to assess cell survival using the MTT assay. As shown in Figure 16, the resulting data created a toxicity profile for carboplatin. The survival responses of each cell line were normalized to the untreated control wells (0 μM concentration of carboplatin) to establish 100% percent cell survival. The amount of cell loss varied both in a concentration and cell-type specific manner. At 50 μM of carboplatin, survival was above 80% cell survival in each cell type, except the HEK293 (grey) (Figure 16). However, at 250 μM concentration, only the MCF7 (royal blue) and HT-29 (pink) cell lines were viable above 60% cell survival (Figure 16). The inhibitory concentration at 50% survival (IC₅₀) differed for each line, reflecting this variability (Table 1). For instance, the SK-MEL-5 IC₅₀ value was within 75 μM ± 4.98 while that of the HT-29 cell line³⁶ was within 350 μM ± 4.23 (Figure 16 and Table 1).

The survival of each cell line decreased differently based on their response to carboplatin (Figure 17). Based on the boxplots, the urinary bladder HT-1197 cell line has decreased cell survival than the breast cancer, MCF7 cell line (Figure 17). There was a significant increase in the HT-29 and MCF7 survival response compared to the control HEK293 cell line (Figure 16). On the other hand, there was no significant difference in the A549, SK-MEL-5, and HT-1197 survival response when compared to the control

HEK293 cell line. This together, the data indicated both a cell type and dose dependent effect after exposure to carboplatin.

Cellular Dose Response to Carboplatin in Multiple Cell Lines

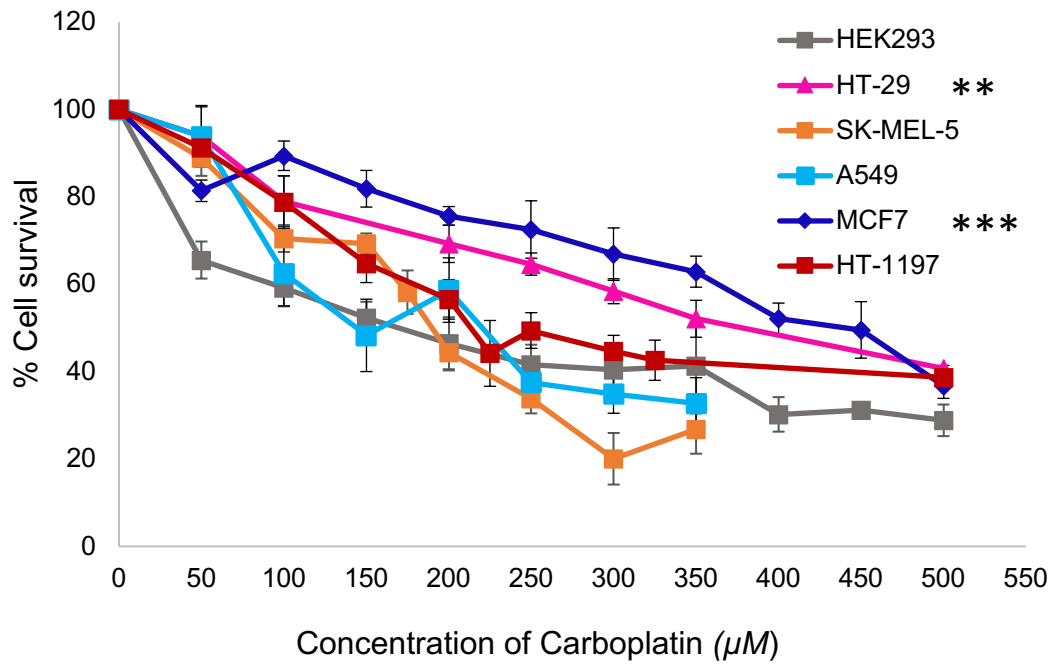


Figure 16. Cellular Dose Response to Carboplatin in Multiple Cell Lines. 750,000 cells were plated for HT-1197 (red); 650,000 cells were plated for HEK293 (grey), and MCF7 (royal blue); 600,000 cells were plated for A549 (aqua blue); 550,000 cells were plated for HT-29 (pink), and SK-MEL-5 (orange) per 24-well plate. For each experiment (n, ± standard error (s.e.)), equal numbers of cells were exposed to increasing concentrations of carboplatin in triplicate for 24 hours. Values are normalized percent cell survival of HT-1197 (n=4), HEK293 (n=9), MCF7 (n=7), A549 (n=5), HT-29 (n=3), and SK-MEL-5 (n=5) in response to varying concentrations of carboplatin. * Represents statistically significant cellular responses in HT-29, SK-MEL-5, A549, MCF7, Ntera2, and HT-1197 cells compared to control HEK293 cells as shown close to their label on the graph (multiple linear regression analysis, ** p <

Carboplatin Survival by Cell Line

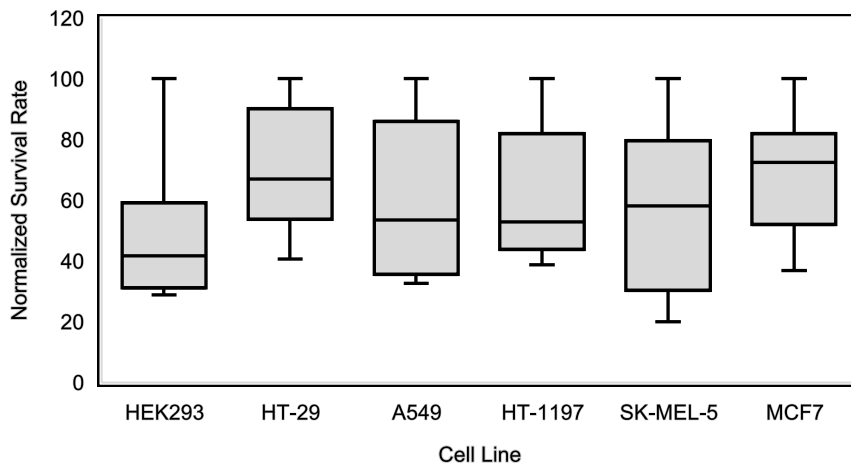


Figure 17. Boxplot representation of normalized survival rate by cell line when exposed to varying concentration of carboplatin. 750,000 cells were plated for HT-1197; 650,000 cells were plated for HEK293, and MCF7; 600,000 cells were plated for A549; 550,000 cells were plated for HT-29, and SK-MEL-5 per 24-well plate. For each experiment ($n \pm$ s.e.), equal numbers of cells were exposed to increasing concentrations of carboplatin in triplicate for 24 hours. Values are normalized percent cell survival of HT-1197 ($n=4$), HEK293 ($n=9$), MCF7 ($n=7$), A549 ($n=5$), HT-29 ($n=3$), and SK-MEL-5 ($n=5$) in response to varying concentrations of carboplatin. The normalized survival rate decreased at different rate depending on the cell line.

3.1.5. IC_{50} Values

The IC_{50} values are used to compare the toxicity of the individual compounds.³⁷

For the colorimetric MTT assay, metabolism is measured by the reduction of the formazan salt and the cell survival is inferred by presence of this activity. Table 1 shows the comparison of the inhibitory concentration at 50% survival (IC_{50}) values in multiple cell lines among platinum (II) compounds. These are the IC_{50} values obtained from experimental data shown in the previous graphs (Figure 10, 12, 14, and 16).

Cell Line	Pt(en)mal	Pt(en)CBDCA	Pt(en)Cl ₂	Carboplatin
HEK293	60 μ M \pm 11.68	50 μ M \pm 5.74	40 μ M	150 μ M \pm 3.69
HT-29	300 μ M \pm 8.77	400 μ M \pm 6.50	250 μ M \pm 4.72	350 μ M \pm 4.23
SK-MEL-5	60 μ M \pm 4.01	100 μ M \pm 8.08	30 μ M \pm 13.63 - 40 μ M \pm 3.60	175 μ M \pm 4.98
A549	350 μ M \pm 3.32	75 μ M \pm 2.78	200 μ M \pm 7.70	200 μ M \pm 7.38
MCF7	80 μ M \pm 5.38	200 μ M \pm 0.98	50 μ M \pm 1.85	400 μ M \pm 3.60
NTERA2	20 μ M \pm 5.61	-	20 μ M \pm 6.26	-
HT-1197	200 μ M \pm 1.78	-	50 μ M \pm 4.20	200 μ M \pm 4.51

Table 1. Comparison of the IC₅₀ shown in (μ M) for each cell line-compound combination. Values are mean of multiple independent experiments \pm standard error (s.e). For each experiment (n), equal numbers of cells were exposed to increasing concentrations of compounds in triplicate for 24 hours. IC₅₀ values for Pt(en)Cl₂+HEK293 (n=1), Pt(en)Cl₂+SK-MEL-5 (between 30 – 40 μ M), and Carboplatin+HT-29 (n=2).

As observed in this table, the IC₅₀ varies for all cell lines and compounds tested. Examining the non-cancerous HEK293 cell line, carboplatin IC₅₀ value (150 μ M \pm 3.69) was higher compared to Pt(en)CBDCA (50 μ M \pm 5.74), indicating lower survival after exposure to the Pt(en)CBDCA compound than carboplatin. Examining each cell line among the three-novel platinum compounds (similar non-leaving ligand structure but varying leaving ligand structure), Pt(en)Cl₂ IC₅₀ value was lower in each cell line compared to Pt(en)mal and Pt(en)CBDCA, except in the small cell lung (A549). Thus, indicating higher survival after exposure to Pt(en)mal and Pt(en)CBDCA compounds compared to Pt(en)Cl₂ (Table 1).

3.2. Effects of Leaving Ligand Differences on Cellular Response

To test the influence of the leaving ligand structure in cytotoxicity, the survival response among the three-novel platinum(II) compounds (Pt(en)mal, Pt(en)CBDCA, and Pt(en)Cl₂) were compared. Using the data from Figure 10 to 15, statistical analysis using multiple linear regression model and t-test was completed.

3.2.1. Effects of Leaving Ligand in HEK293 Cell Line

Data from the concentration response curves for the non-cancerous cells HEK 293 were analyzed to examine the effects of the non-leaving ligand. HEK 293 as shown in Figure 18 illustrates normalized survival responses at 0 μM , 50 μM , 100 μM and 200 μM concentrations for Pt(en)mal, Pt(en)CBDCA, and Pt(en)Cl₂ compounds. Pt(en)Cl₂ (yellow, $\text{IC}_{50} = 40 \mu\text{M}$) showed significant decrease in survival compared to Pt(en)mal (orange, $\text{IC}_{50} = 60 \mu\text{M} \pm 11.68$) and Pt(en)CBDCA (blue, $\text{IC}_{50} = 50 \mu\text{M} \pm 5.74$) (Table 1 and Figure 18) in HEK293 cells. The effect was also seen at 50 μM (p-value < 0.001 at 95% CI), 100 μM (p-value = 0.001 at 95% CI) and 200 μM (p-value was 0.041 at 95% CI) concentrations when Pt(en)Cl₂ was compared to Pt(en)mal. However, there was no significant difference in response between Pt(en)CBDCA and Pt(en)mal at the three concentrations in the HEK293 cell line (Figure 18).

Effects of Leaving Ligand in HEK293 Cell Line

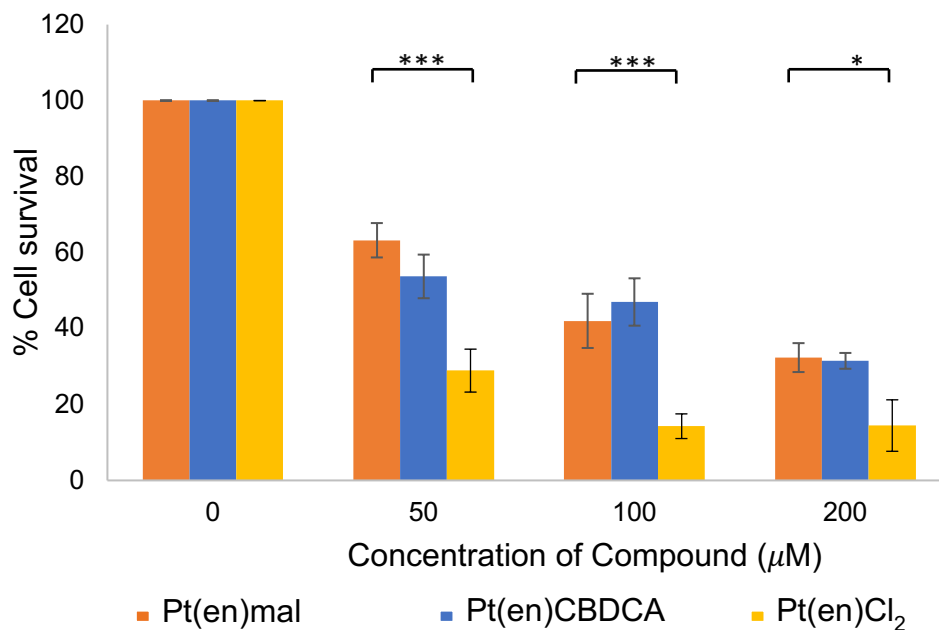


Figure 18. Effects of Leaving Ligand in Human Embryonic Kidney (HEK293) cells. 650,000 cells were plated for HEK293 per 24-well plate. Values are normalized percent cell survival of HEK293 cell line in response to Pt(en)mal (n=8, \pm s.e.), Pt(en)CBDCA (n=8, \pm s.e.), and Pt(en)Cl₂ (n=5, \pm s.e.) at 0 μ M, 50 μ M, 100 μ M, and 200 μ M concentrations after 24 hours incubation. Orange denotes Pt(en)mal; blue denotes Pt(en)CBDCA; and yellow denotes Pt(en)Cl₂. * Represents statistically significant survival responses in Pt(en)CBDCA and Pt(en)Cl₂ compared to Pt(en)mal at 0 μ M as shown on the graph (multiple linear regression analysis, * p < 0.05, ** p < 0.01, *** p < 0.001).

3.2.2. Effects of Leaving Ligand in HT-29 Cell Line

Data from the concentration response curves for the colorectal adenocarcinoma (HT-29) were also analyzed to examine the effects of the non-leaving ligand. The normalized survival responses of HT-29 cells were at 0 μ M, 100 μ M, 250 μ M and 500 μ M concentrations for Pt(en)mal, Pt(en)CBDCA, and Pt(en)Cl₂ compounds (Figure 19).

Effects of Leaving Ligand in HT-29 Cell Line

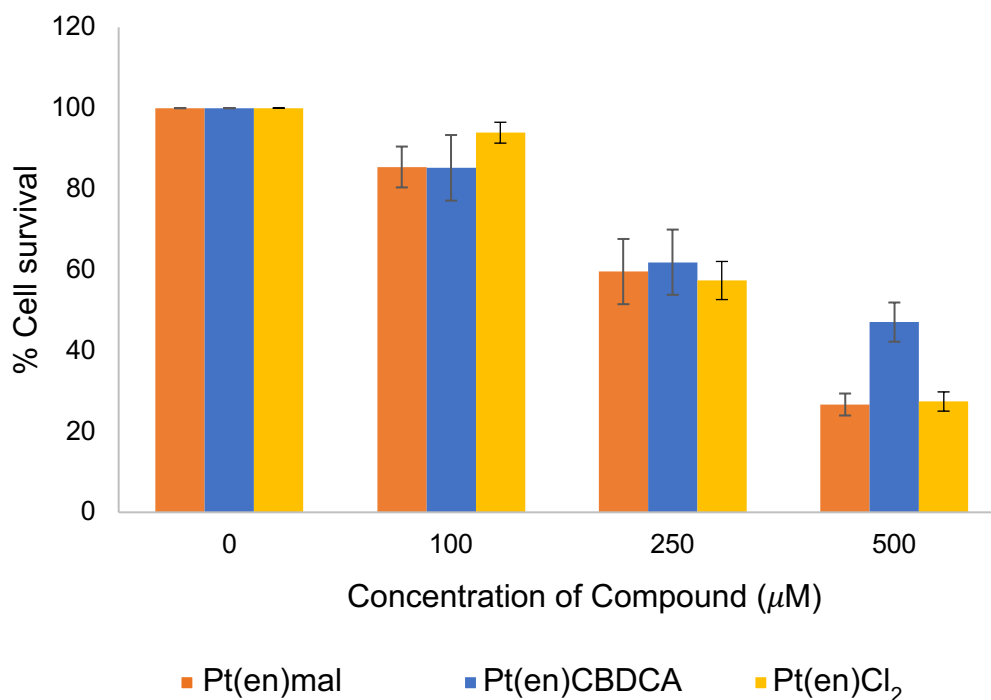


Figure 19. Effects of Leaving Ligand in Colorectal adenocarcinoma (HT-29) Cell Line. 650,000 cells were plated for HT-29 per 24-well plate. Values are normalized percent cell survival of HT-29 cell line in response to Pt(en)mal (n=5, \pm s.e.), Pt(en)CBDCA (n=7, \pm s.e.), and Pt(en)Cl₂ (n=5, \pm s.e.) at 0 μ M, 50 μ M, 100 μ M, and 200 μ M concentrations after 24 hours incubation. Orange denotes Pt(en)mal; blue denotes Pt(en)CBDCA; and yellow denotes Pt(en)Cl₂. * Represents statistically significant survival responses in Pt(en)CBDCA and Pt(en)Cl₂ compared to Pt(en)mal at 0 μ M as shown on the graph (multiple linear regression analysis, * p < 0.05, ** p < 0.01, *** p < 0.001).

In the colorectal HT-29 cell line, all three compounds, Pt(en)mal (orange, IC₅₀ = 300 μ M \pm 8.77), Pt(en)CBDCA (blue, IC₅₀ = 400 μ M \pm 6.50), and Pt(en)Cl₂ (yellow, IC₅₀ = 250 μ M \pm 4.72) indicated less toxicity compared to the non-cancerous HEK293 cell

line (Figure 19 and Table 1). Additionally, there was no statistically significant difference in survival response at 100 μM , 250 μM , and 500 μM concentrations between the three ethylenediamine (en) non-leaving ligand compound (Figure 19). Even at 500 μM concentration, no significant effect was determined.

3.2.3. Effects of Leaving Ligand in A549 Cell Line

Data from the concentration response curves for the small cell lung carcinoma (A549) were analyzed to examine the effects of the non-leaving ligand. Figure 20 illustrates the normalized survival responses of A549 cell lines normalized to untreated wells at 0 μM , 50 μM , 100 μM and 300 μM concentrations for Pt(en)mal, Pt(en)CBDCA, and Pt(en)Cl₂ compounds. In the small cell lung, A549 cell line, there was a significant difference in cell survival response to Pt(en)CBDCA (blue) at 50 μM (p-value < 0.001 at 95% CI) and 100 μM (p-value < 0.001 at 95% CI) concentrations compared to Pt(en)mal (orange) (Figure 20). At 300 μM concentration, the p-value of 0.013 (at 95% CI) in Pt(en)CBDCA indicated a significant difference in survival response than in Pt(en)mal. Percent cell survival decreased in Pt(en)CBDCA ($\text{IC}_{50} = 75 \mu\text{M} \pm 2.78$) compared to the Pt(en)mal ($\text{IC}_{50} = 350 \mu\text{M} \pm 3.32$) and Pt(en)Cl₂ ($\text{IC}_{50} = 200 \mu\text{M} \pm 7.70$) compounds in the A549 cell line (Figure 20). There was only a significant difference in A549 survival response to Pt(en)Cl₂ (yellow) at 300 μM (p-value 0.012 at 95% CI) compared to Pt(en)mal (Figure 20).

Effects of Leaving Ligand in A549 Cell Line

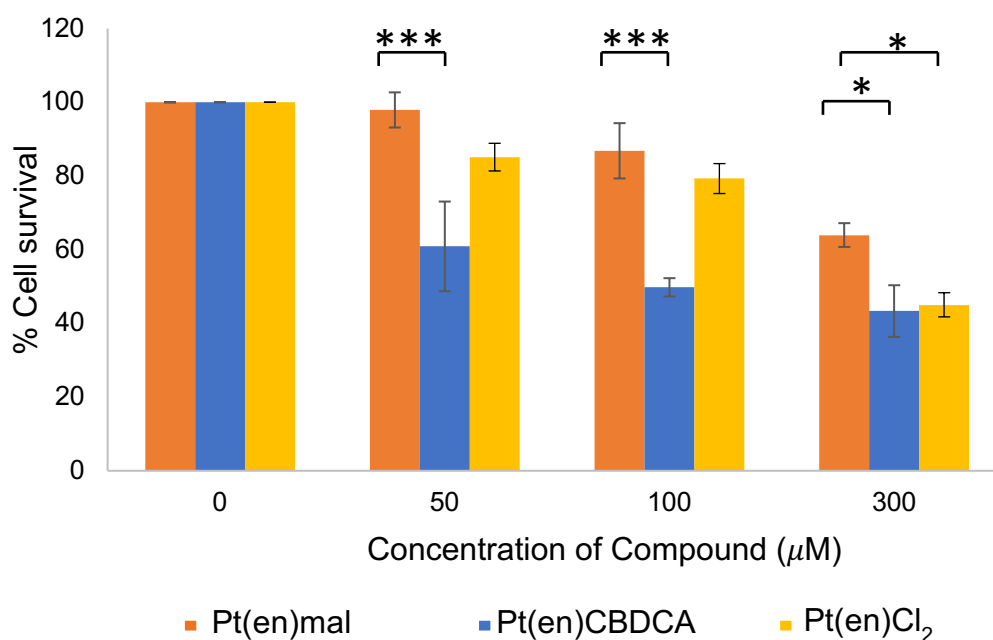


Figure 20. Effects of Leaving Ligand in Small Cell Lung Carcinoma (A549) Cell Line. 550,000 cells were plated for A549 in Pt(en)mal; 550,000 to 600,000 cells were plated for A549 in Pt(en)CBDCA, and 650,000 cells were plated for A549 in Pt(en)Cl₂ per 24-well plate. Values are normalized percent cell survival of A549 cell line in response to Pt(en)mal (n=13, ± s.e.), Pt(en)CBDCA (n=4, ± s.e.), Pt(en)Cl₂ (n=4, ± s.e.) at 0 µM, 50 µM, 100 µM, and 200 µM concentrations after 24 hours incubation. Orange denotes Pt(en)mal; blue denotes Pt(en)CBDCA; and yellow denotes Pt(en)Cl₂. * Represents statistically significant survival responses in Pt(en)CBDCA and Pt(en)Cl₂ compared to Pt(en)mal at 0µM as shown on the graph (multiple linear regression analysis, * p < 0.05, ** p < 0.01, *** p < 0.001).

3.2.4. Effect of Leaving Ligand in SK-MEL-5 Cell line

Data from the concentration response curves for the melanoma (SK-MEL-5) were analyzed to examine the effects of the non-leaving ligand. As shown in Figure 21, the normalized survival responses of SK-MEL-5 cell lines at 0 µM, 20 µM, 60 µM and 100

μM concentrations for Pt(en)mal, Pt(en)CBDCA, and Pt(en)Cl₂ compounds were compared.

Effects of Leaving Ligand in SK-MEL-5 Cell Line

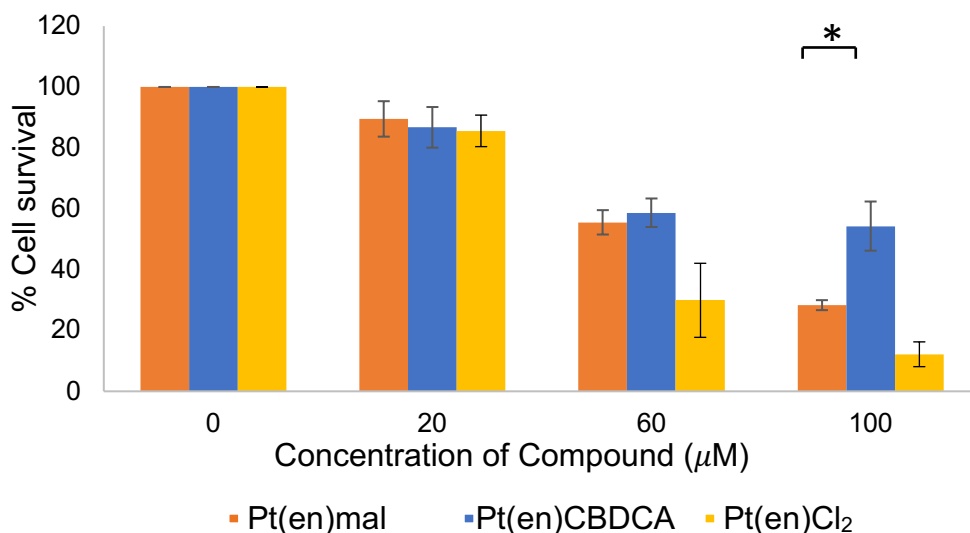


Figure 21. Effects of Leaving Ligand in Melanoma (SK-MEL-5) Cell Line. 550,000 cells were plated for SK-MEL-5 in Pt(en)mal and Pt(en)Cl₂; 650,000 cells were plated for SK-MEL-5 in Pt(en)CBDCA per 24-well plate. Values are normalized percent cell survival of SK-MEL-5 cell line in response to Pt(en)mal (n=4, \pm s.e.), Pt(en)CBDCA (n=8, \pm s.e.), and Pt(en)Cl₂ (n=3, \pm s.e.) at 0 μM , 50 μM , 100 μM , and 200 μM concentrations after 24 hours incubation. Orange denotes Pt(en)mal; blue denotes Pt(en)CBDCA; and yellow denotes Pt(en)Cl₂. * Represents statistically significant survival responses in Pt(en)CBDCA and Pt(en)Cl₂ compared to Pt(en)mal at 0 μM as shown on the graph (multiple linear regression analysis, * p < 0.05, ** p < 0.01, *** p < 0.001).

In the melanoma (SK-MEL-5) cell line, the three (en) non-leaving ligand compounds showed higher toxicity at increased concentrations (Figure 21). At 20 μM and 60 μM concentrations, there was no statistical difference in cell survival between

Pt(en)mal (orange), Pt(en)CBDCA (blue), and Pt(en)Cl₂ (yellow). However, there was a significant difference in SK-MEL-5 response to Pt(en)CBDCA at 100 μ M (p-value 0.023 at 95% CI) concentration when compared to Pt(en)mal (Figure 21). At same 100 μ M concentration, there was no significant difference in SK-MEL-5 survival response found between Pt(en)mal and Pt(en)Cl₂.

3.2.4. Effects of Leaving Ligand in HT-1197 Cell Line

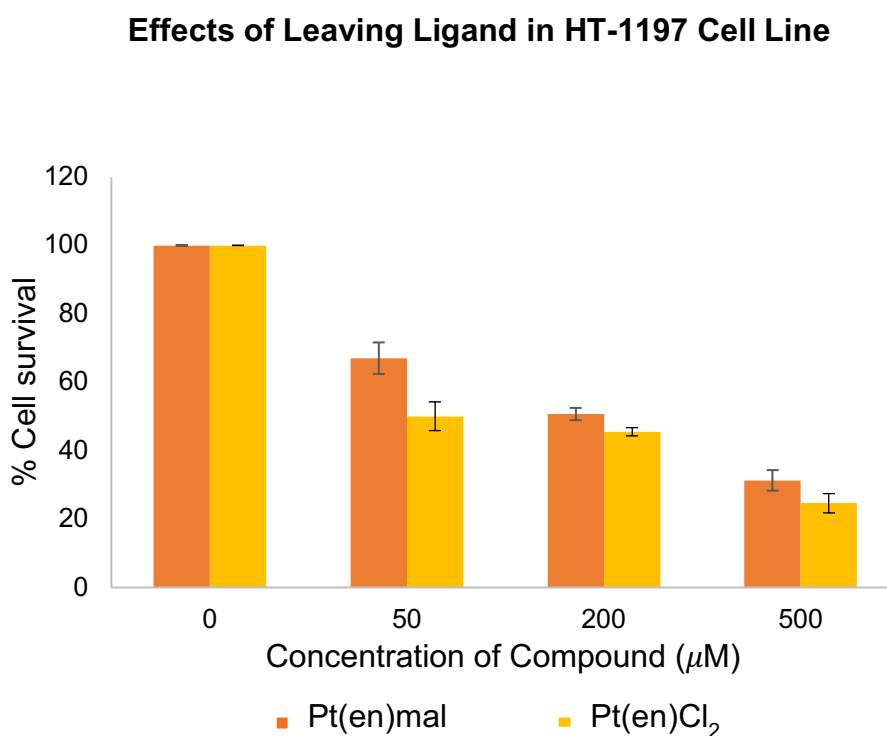


Figure 22. Effects of Leaving Ligand in Urinary Bladder Carcinoma (HT-1197) Cell Line. 750,000 cells were plated for HT-1197 in Pt(en)mal and Pt(en)Cl₂ per 24-well plate. Values are normalized percent cell survival of HT-1197 cell line in response to Pt(en)mal (n=3, \pm s.e.), and Pt(en)Cl₂ (n=6, \pm s.e.) at 0 μ M, 50 μ M, 200 μ M, and 500 μ M concentrations after 24 hours incubation. Orange denotes Pt(en)mal; and yellow denotes Pt(en)Cl₂. * Represents statistically significant survival responses in Pt(en)Cl₂ compared to Pt(en)mal at 0 μ M as shown on the graph (t-test analysis, * p < 0.05, ** p < 0.01, *** p < 0.001).

In urinary bladder carcinoma (HT-1197), the examination of the effects of the non-leaving ligand at 0 μM , 50 μM , 200 μM and 500 μM concentrations were examined for Pt(en)mal, and Pt(en)Cl₂ compounds (Figure 22). In the urinary bladder HT-1197 cell line, there was less toxicity to Pt(en)Cl₂ (yellow, IC₅₀ = 50 μM \pm 4.20) compared to Pt(en)mal (orange, IC₅₀ = 200 μM \pm 1.78) (Figure 22). Additionally, there was no statistically significant difference in survival response at 50 μM , 200 μM , and 500 μM concentrations between the two ethylenediamine (en) non-leaving ligand compound (Figure 22).

3.2.5. Effects of Leaving Ligand in NTERA2 Cell Line

Data from the concentration response curves for the human testicular embryonic carcinoma (NTERA2) were analyzed to examine the effects of the non-leaving ligand. The normalized survival responses of NTERA2 cell lines 0 μM , 20 μM , 40 μM and 100 μM concentrations for Pt(en)mal, and Pt(en)Cl₂ compounds (Figure 23) was compared. Pt(en)mal (IC₅₀ = 20 μM \pm 5.61), and Pt(en)Cl₂ (IC₅₀ = 20 μM \pm 6.26) indicated higher toxicity even at 100 μM concentrations in the testicular Ntera2 cell line (Figure 23). However, there was no significant difference in survival response at 20 μM , 40 μM , and 100 μM concentrations between the two ethylenediamine (en) non-leaving ligand compound (Figure 23).

Effects of Leaving Ligand in NTERA2 Cell Line

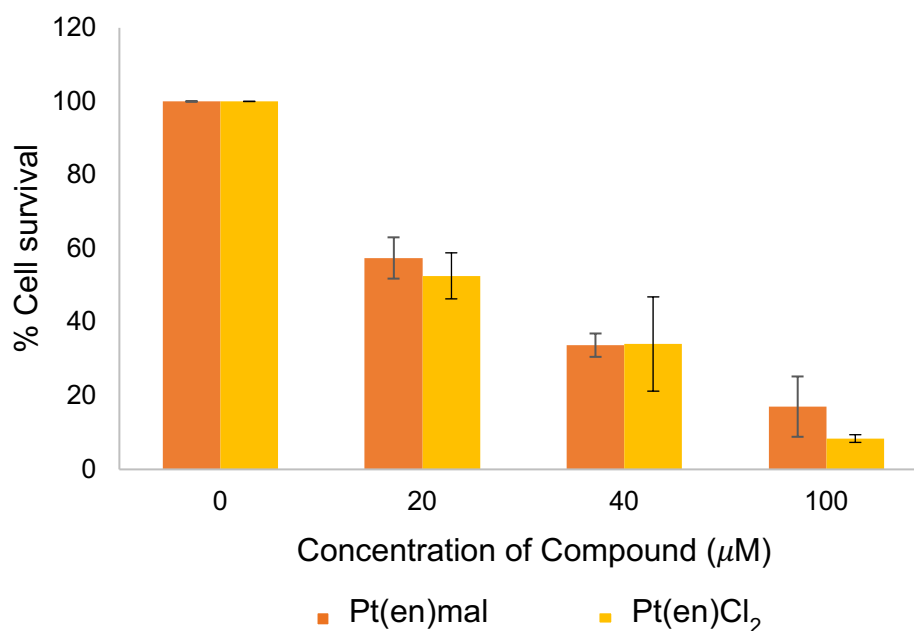


Figure 23. Effects of Leaving Ligand in Human Testicular Embryonic Carcinoma (NTERA2) Cell Line. 650,000 cells were plated for Ntera2 in Pt(en)mal and Pt(en)Cl₂ per 24-well plate. Values are normalized percent cell survival of Ntera2 cell line in response to Pt(en)mal (n=6, ± s.e.), and Pt(en)Cl₂ (n=5, ± s.e.) at 0 µM, 20 µM, 40 µM, and 100 µM concentrations after 24 hours incubation. Orange denotes Pt(en)mal; and yellow denotes Pt(en)Cl₂. * Represents statistically significant survival responses in Pt(en)Cl₂ compared to Pt(en)mal at 0µM as shown on the graph (t-test analysis, * p < 0.05, ** p < 0.01, *** p < 0.001).

4. DISCUSSION

In this study, we hypothesized that the cell survival response of platinum(II) compounds varies due to structural differences in the leaving ligands. To test this hypothesis, we examined the cell survival response after individual exposure to increasing concentrations of three novel platinum(II) compounds: Pt(en)mal, Pt(en)CBDCA, and Pt(en)Cl₂. These novel platinum compounds possess same ethylenediamine (en) non-leaving ligands but different leaving ligands – malonate (mal),

1,1-cyclobutanedicarboxylic acid (CBDCA) (the carboplatin leaving ligand), and dichloride (Cl_2) (the cisplatin leaving ligand) respectively. Based on the findings, there was strong evidence of cell line effect for each compound.

Platinum(II) compounds including novel Pt(en)mal, Pt(en)CBDCA, Pt(en) Cl_2 survival response is cell type specific. For the Pt(en)mal survival response, the small cell lung A549, colorectal HT-29, and urinary bladder HT-1197 cell lines displayed significantly higher percent cell survival while the testicular NTERA2 cell line showed significantly lower percent cell survival compared to the non-cancerous control HEK293 cell line (Figure 10). This indicated that there was less toxicity in the A549, HT-29, and HT-1197 cell lines while higher toxicity in the testicular NTERA2 cells when exposed to Pt(en)mal compared to the other cell lines. For the Pt(en)CBDCA survival response, data reflects a significantly higher percent cell survival in the colorectal HT-29 and breast MCF7 cell lines compared to the control HEK293 cells (Figure 12). The HT-29 was the most prominent in survival response when comparing with the other cell lines. As expected, similar survival response was found in the FDA-approved chemotherapeutic carboplatin data (Figure 16). However, the breast MCF7 was the most prominent when comparing with the other cell lines in carboplatin survival response. Pt(en)CBDCA is structurally like carboplatin, which is not the most effective treatment for colon, colorectal, or breast cancers. Therefore, the lower toxicity of HT-29 and MCF7 to Pt(en)CBDCA compared to the other cell lines was to be expected.

Data also suggests a cell line effects in Pt(en) Cl_2 , and it was more prominent when comparing HT-29 and A549 to the other cell lines. Additionally, there was a significantly increase in cell survival in the colorectal HT-29, small cell lung A549, and urinary

bladder HT-1197 survival response to Pt(en)Cl₂ when compared to the control HEK293 cell line (Figure 14). Pt(en)Cl₂ is structurally similar to cisplatin, as they both share similar dichloride leaving ligand structure but different non-leaving ligand. Cisplatin is most effective for the treatment of testicular cancer, though it is also used as first line treatment for small cell lung and ovarian cancer.^{2,4,10} Therefore, the significant difference between HT-29 and HT-1197 survival response and the other cell lines in Pt(en)Cl₂ was expected except for the small cell lung A549 cell line.

Though, non-leaving ligands play crucial role in altering the reactivity of aqua platinum species with biological target DNA.^{2,10} The role of leaving ligands, which are substituted by the biological target DNA, is yet to be understood. In our study, we focused on the effect of leaving ligands in specific cell lines. Here, the influence of the leaving ligand structure on cell survival was examined by comparing cell survival response among the three novel platinum compounds (Pt(en)mal, Pt(en)CBDCA, and Pt(en)Cl₂) in specific cell types. In the HEK293 cell line, our data showed concentration dependent decrease in cell survival among the three (en) non-leaving ligand compounds (Figure 18). Our data indicated higher toxicity of Pt(en)Cl₂ in HEK293 non-cancerous cell line compared to Pt(en)mal and Pt(en)CBDCA (Figure 18). In the colorectal HT-29 cell line, there was a concentration dependent effect on cell survival among the three (en) non-leaving ligand compounds (Figure 19) as expected. However, the IC₅₀ was observed among the three compounds. Based on our data, it was indicated that all three (en) compounds exhibited lower toxicity even at higher concentrations in the colorectal HT-29 cell lines (Figure 19).

In the small cell lung A549 cell line, a concentration dependent decrease was also observed among the three (en) non-leaving ligand compounds (Figure 20). Pt(en)CBDCA showed significantly lower survival response both at lower and higher concentrations in the A549 compared to Pt(en)mal. In contrast, Pt(en)mal and Pt(en)Cl₂ showed similar survival responses except at high concentrations. In particular, there was a significant difference in survival response between Pt(en)mal and Pt(en)Cl₂ at 300 μ M concentration (Figure 20). Based on findings, Pt(en)CBDCA seems to exhibit higher toxicity in the small cell lungs compared to the other (en) compounds. In the melanoma SK-MEL-5 cell line, the three (en) non-leaving ligand compounds also showed concentration dependent effect on cell survival (Figure 21) as expected. There were similar survival responses among all three compounds except at 100 μ M concentration, where Pt(en)CBDCA showed a significant increase in survival response compared to the other (en) compounds. This suggests that Pt(en)CBDCA is less toxic to the melanoma SK-MEL-5 cell-type when exposed at higher concentrations compared to Pt(en)mal and Pt(en)Cl₂.

For both the urinary bladder HT-1197 and testicular NTERA2 cell line, only the Pt(en)mal and Pt(en)Cl₂ compounds were compared due to available data. In the urinary bladder HT-1197, there was a concentration dependent decrease seen among Pt(en)mal and Pt(en)Cl₂. However, the two (en) non-leaving ligands showed similar survival response (Figure 22). In the testicular NTERA2 cell line, the two compounds were toxic at lower concentrations. Both (en) non-leaving ligands also showed similar survival response in NTERA2 cell line. Overall, the summary of the inhibitory concentration at 50% survival (IC₅₀) showed varying toxicity of the platinum compounds between each

cell lines (Table 1). Pt(en)Cl₂ exhibited highest toxicity in each cell lines compared to Pt(en)mal and Pt(en)CBDCA except in the small cell lung A549 cell line.

5. CONCLUSION

Though, extensive studies have shown that platinum(II) compounds and cell type possess same mechanism of platinum initiating cell deaths, why these platinum(II) compounds target specific tissue of cancer origin remain unclear. In our study, we proposed that the cell survival response of these platinum(II) compounds vary due to structural differences in the leaving ligands. Thereby, we focused on the effect of leaving ligands in specific cell lines. Data from the concentration response curve indicated less toxicity in Pt(en)mal, Pt(en)CBDCA, and Pt(en)Cl₂ even at higher concentrations in the colorectal HT-29 cell line compared to the non-cancerous HEK293 cell line (Figure 18 and 19). However, data showed higher toxicity in Pt(en)CBDCA when compared to the other two novel platinum compounds in the small cell lung carcinoma (A549) cell line. Given the differences in inhibitory concentration at 50% survival (IC₅₀) as shown in Table 1, we therefore conclude that both leaving ligand structures and cell types influences cell survival response of platinum(II) compounds.

6. FUTURE DIRECTION

Although the mechanism of toxicity for platinum(II) compounds has been studied, little is known about the transport of the platinum compounds both in (uptake) and out (efflux) of the cell, and what effect this has on cytotoxicity. To best understand the influence of cellular transport on cytotoxicity, it is important to first understand the mechanism of metal transports. Therefore, in future studies, we aim to determine intracellular concentrations of platinum using atomic absorption spectrometer (AAS) in

multiple cell lines at similar levels of survival to compare their cellular response to intracellular platinum concentrations. Given that transporters are mediators between platinum toxicity and cell survival, we will examine the expression levels of potential platinum transporters such as the organic cation transporters (OCT1 and OCT2)^{1,2,28}, and copper transporter receptor-1 (CTR1)^{38,39} in different cell lines using western blot analysis or cell staining. The basal transporter expression levels will be analyzed in different cell lines and then the transporter expression levels after exposure to platinum compounds will also be determined. Our overall goal is to provide clear understanding on the structural impact of leaving ligands to cellular toxicity.

REFERENCES

- (1) Qi, L.; Luo, Q.; Zhang, Y.; Jia, F.; Zhao, Y.; Wang, F. Advances in Toxicological Research of the Anticancer Drug Cisplatin. *Chem. Res. Toxicol.* **2019**, *32* (8), 1469–1486.
- (2) Wang, D.; Lippard, S. J. Cellular Processing of Platinum Anticancer Drugs. *Nat. Rev. Drug Discov.* **2005**, *4* (4), 307–320.
- (3) ROSENBERG, B.; VANCAMP, L.; TROSKO, J. E.; MANSOUR, V. H. Platinum Compounds: A New Class of Potent Antitumour Agents. *Nature* **1969**, *222* (5191), 385–386.
- (4) Jung, Y.; Lippard, S. J. Direct Cellular Responses to Platinum-Induced DNA Damage. *Chem. Rev.* **2007**, *107* (5), 1387–1407.
- (5) Browning, R. J.; Reardon, P. J. T.; Parhizkar, M.; Pedley, R. B.; Edirisinghe, M.; Knowles, J. C.; Stride, E. Drug Delivery Strategies for Platinum-Based Chemotherapy. *ACS Nano* **2017**, *11* (9), 8560–8578.
- (6) Eastman, A. The Formation, Isolation and Characterization of DNA Adducts Produced by Anticancer Platinum Complexes. *Pharmacol. Ther.* **1987**, *34* (2), 155–166.
- (7) Kauffman, G. B.; Pentimalli, R.; Doldi, S.; Hall, M. D. Michele Peyrone (1813-1883), Discoverer of Cisplatin. *Platin. Met. Rev.* **2010**, *54* (4), 250–256.
- (8) ROSENBERG, B.; VAN CAMP, L.; KRIGAS, T. Inhibition of Cell Division in Escherichia Coli by Electrolysis Products from a Platinum Electrode. *Nature* **1965**, *205* (4972), 698–699.

- (9) Rosenberg, B.; VanCamp, L. The Successful Regression of Large Solid Sarcoma 180 Tumors by Platinum Compounds. *Cancer Res.* **1970**, *30* (6), 1799–1802.
- (10) Boulikas, T.; Pantos, A.; Bellis, E.; Christofis, P. Designing Platinum Compounds in Cancer: Structures and Mechanisms. *Cancer Ther.* **2007**, *5*, 537–583.
- (11) Kelland, L. The Resurgence of Platinum-Based Cancer Chemotherapy. *Nat. Rev. Cancer* **2007**, *7* (8), 573–584.
- (12) Rottenberg, S.; Disler, C.; Perego, P. The Rediscovery of Platinum-Based Cancer Therapy. *Nat. Rev. Cancer* **2021**, *21* (1), 37–50.
- (13) Meijer, C.; Mulder, N. H.; Timmer-Bosscha, H.; Sluiter, W. J.; Meersma, G. J.; de Vries, E. G. E. Relationship of Cellular Glutathione to the Cytotoxicity and Resistance of Seven Platinum Compounds. *Cancer Res.* **1992**, *52* (24), 6885.
- (14) Chaney, S. G.; Campbell, S. L.; Bassett, E.; Wu, Y. Recognition and Processing of Cisplatin- and Oxaliplatin-DNA Adducts. *Crit. Rev. Oncol. Hematol.* **2005**, *53* (1), 3–11.
- (15) Kartalou, M.; Essigmann, J. M. Recognition of Cisplatin Adducts by Cellular Proteins. *Mutat. Res. Mol. Mech. Mutagen.* **2001**, *478* (1–2), 1–21.
- (16) Damsma, G. E.; Alt, A.; Brueckner, F.; Carell, T.; Cramer, P. Mechanism of Transcriptional Stalling at Cisplatin-Damaged DNA. *Nat. Struct. Mol. Biol.* **2007**, *14* (12), 1127–1133.
- (17) Qi, L.; Luo, Q.; Zhang, Y.; Jia, F.; Zhao, Y.; Wang, F. Advances in Toxicological Research of the Anticancer Drug Cisplatin. *Chem. Res. Toxicol.* **2019**, *32* (8), 1469–1486.

- (18) Cheng, Y.; El-Kattan, A.; Zhang, Y.; Ray, A. S.; Lai, Y. Involvement of Drug Transporters in Organ Toxicity: The Fundamental Basis of Drug Discovery and Development. *Chem. Res. Toxicol.* **2016**, *29* (4), 545–563.
- (19) Wang, D.; Lippard, S. J. Cellular Processing of Platinum Anticancer Drugs. *Nat. Rev. Drug Discov.* **2005**, *4* (4), 307–320.
- (20) Planells-Cases, R.; Lutter, D.; Guyader, C.; Gerhards, N. M.; Ullrich, F.; Elger, D. A.; Kucukosmanoglu, A.; Xu, G.; Voss, F. K.; Reincke, S. M. Subunit Composition of VRAC Channels Determines Substrate Specificity and Cellular Resistance to P T-based Anti-cancer Drugs. *EMBO J.* **2015**, *34* (24), 2993–3008.
- (21) Harrach, S.; Ciarimboli, G. Role of Transporters in the Distribution of Platinum-Based Drugs. *Front. Pharmacol.* **2015**, *6*, 85.
- (22) Ciarimboli, G.; Deuster, D.; Knief, A.; Sperling, M.; Holtkamp, M.; Edemir, B.; Pavenstädt, H.; Lanvers-Kaminsky, C.; am Zehnhoff-Dinnesen, A.; Schinkel, A. H.; Koepsell, H.; Jürgens, H.; Schlatter, E. Organic Cation Transporter 2 Mediates Cisplatin-Induced Oto- and Nephrotoxicity and Is a Target for Protective Interventions. *Am. J. Pathol.* **2010**, *176* (3), 1169–1180.
- (23) Ciarimboli, G.; Ludwig, T.; Lang, D.; Pavenstädt, H.; Koepsell, H.; Piechota, H.-J.; Haier, J.; Jaehde, U.; Zisowsky, J.; Schlatter, E. Cisplatin Nephrotoxicity Is Critically Mediated via the Human Organic Cation Transporter 2. *Am. J. Pathol.* **2005**, *167* (6), 1477–1484.
- (24) Townsend, D. M.; Deng, M.; Zhang, L.; Lapus, M. G.; Hanigan, M. H. Metabolism of Cisplatin to a Nephrotoxin in Proximal Tubule Cells. *J. Am. Soc. Nephrol.* **2003**, *14* (1), 1.

- (25) Farrell, N.; Qu, Y.; Hacker, M. P. Cytotoxicity and Antitumor Activity of Bis (Platinum) Complexes. A Novel Class of Platinum Complexes Active in Cell Lines Resistant to Both Cisplatin and 1, 2-Diaminocyclohexane Complexes. *J. Med. Chem.* **1990**, *33* (8), 2179–2184.
- (26) Wee, N. K. Y.; Weinstein, D. C.; Fraser, S. T.; Assinder, S. J. The Mammalian Copper Transporters CTR1 and CTR2 and Their Roles in Development and Disease. *Int. J. Biochem. Cell Biol.* **2013**, *45* (5), 960–963.
<https://doi.org/10.1016/j.biocel.2013.01.018>.
- (27) Tiong, H. Y.; Huang, P.; Xiong, S.; Li, Y.; Vathsala, A.; Zink, D. Drug-Induced Nephrotoxicity: Clinical Impact and Preclinical in Vitro Models. *Mol. Pharm.* **2014**, *11* (7), 1933–1948.
- (28) Zhang, S.; Lovejoy, K. S.; Shima, J. E.; Lagpacan, L. L.; Shu, Y.; Lapuk, A.; Chen, Y.; Komori, T.; Gray, J. W.; Chen, X.; Lippard, S. J.; Giacomini, K. M. Organic Cation Transporters Are Determinants of Oxaliplatin Cytotoxicity. *Cancer Res.* **2006**, *66* (17), 8847–8857.
- (29) Nakamura, T.; Yonezawa, A.; Hashimoto, S.; Katsura, T.; Inui, K. Disruption of Multidrug and Toxin Extrusion MATE1 Potentiates Cisplatin-Induced Nephrotoxicity. *Biochem. Pharmacol.* **2010**, *80* (11), 1762–1767.
- (30) Browning, R. J.; Reardon, P. J. T.; Parhizkar, M.; Pedley, R. B.; Edirisinghe, M.; Knowles, J. C.; Stride, E. Drug Delivery Strategies for Platinum-Based Chemotherapy. *ACS Nano* **2017**, *11* (9), 8560–8578.
- (31) Litterst, C. L.; Gram, T. E.; Dedrick, R. L.; Leroy, A. F.; Guarino, A. M. Distribution and Disposition of Platinum Following Intravenous Administration of

- Cis-Diamminedichloroplatinum(II) (NSC 119875) to Dogs. *Cancer Res.* **1976**, *36* (7), 2340–2344.
- (32) Bulacio, R. P.; Anzai, N.; Ouchi, M.; Torres, A. M. Organic Anion Transporter 5 (Oat5) Urinary Excretion Is a Specific Biomarker of Kidney Injury: Evaluation of Urinary Excretion of Exosomal Oat5 after N-Acetylcysteine Prevention of Cisplatin Induced Nephrotoxicity. *Chem. Res. Toxicol.* **2015**, *28* (8), 1595–1602.
- (33) Samimi, G.; Safaei, R.; Katano, K.; Holzer, A. K.; Rochdi, M.; Tomioka, M.; Goodman, M.; Howell, S. B. Increased Expression of the Copper Efflux Transporter ATP7A Mediates Resistance to Cisplatin, Carboplatin, and Oxaliplatin in Ovarian Cancer Cells. *Clin. Cancer Res.* **2004**, *10* (14), 4661.
- (34) van Meerloo, J.; Kaspers, G. J. L.; Cloos, J. Cell Sensitivity Assays: The MTT Assay. In *Cancer Cell Culture*; Cree, I. A., Ed.; Methods in Molecular Biology; Humana Press: Totowa, NJ, **2011**, *731*, 237–245.
- (35) Kuete, V.; Karosmanoglu, O.; Sivas, H. Anticancer Activities of African Medicinal Spices and Vegetables. In *Medicinal Spices and Vegetables from Africa*, **2017**, 271–297.
- (36) Veletanlic, V. Toxicity of Novel Platinum Compounds in Mammalian Cancer Cells. Thesis, *Western Kentucky University, Department of Chemistry*, **2020**, 1-29.
- (37) Berrouet, C.; Dorilas, N.; Rejniak, K. A.; Tuncer, N. Comparison of Drug Inhibitory Effects (IC₅₀) in Monolayer and Spheroid Cultures. *Bull. Math. Biol.* **2020**, *82* (6), 68.

- (38) Lee, Y.-Y. Prognostic Value of the Copper Transporters, CTR1 and CTR2, in Patients with Ovarian Carcinoma Receiving Platinum-Based Chemotherapy. *Gynecol. Oncol.* **2011**, *122* (2), 361–365.
- (39) Chen, H. H. W.; Yan, J.-J.; Chen, W.-C.; Kuo, M. T.; Lai, Y.-H.; Lai, W.-W.; Liu, H.-S.; Su, W.-C. Predictive and Prognostic Value of Human Copper Transporter 1 (HCtr1) in Patients with Stage III Non-Small-Cell Lung Cancer Receiving First-Line Platinum-Based Doublet Chemotherapy. *Lung Cancer* **2012**, *75* (2), 228–234.